

ВЦЗЗЭДЯУОШНКА



AIAA
DESIGN/BUILD/FLY
2015-2016
DESIGN REPORT



Georgia Institute
of **Tech**nology®



TABLE OF CONTENTS

1. EXECUTIVE SUMMARY	4
1.1 DESIGN PROCESS	4
1.2 KEY MISSION REQUIREMENTS AND DESIGN FEATURES	4
1.3 PERFORMANCE CAPABILITIES OF THE SYSTEM	5
2. MANAGEMENT SUMMARY	6
2.1 TEAM ORGANIZATION	6
2.2 MILESTONE CHART	7
3. CONCEPTUAL DESIGN.....	7
3.1 MISSION REQUIREMENTS	7
3.2 TRANSLATION INTO DESIGN REQUIREMENTS	13
3.3 CONFIGURATIONS CONSIDERED	15
3.4 COMPONENT WEIGHTING AND SELECTION PROCESS.....	16
3.5 FINAL CONCEPTUAL DESIGN CONFIGURATION	17
4. PRELIMINARY DESIGN	19
4.1 DESIGN METHODOLOGY	19
4.2 DESIGN TRADES.....	19
4.3 MISSION MODEL.....	22
4.4 AERODYNAMIC CHARACTERISTICS	22
4.5 STABILITY AND CONTROL.....	27
4.6 MISSION PERFORMANCE	29
5. DETAIL DESIGN.....	30
5.1 FINAL DESIGN	30
5.2 STRUCTURAL CHARACTERISTICS	31
5.3 SYSTEM AND SUBSYSTEM DESIGN/COMPONENT/SELECTION/INTEGRATION	33
5.4 WEIGHT AND BALANCE	37
5.5 FLIGHT AND MISSION PERFORMANCE	38
5.6 DRAWING PACKAGE	41
6. MANUFACTURING PLAN AND PROCESSES.....	47
6.1 MANUFACTURING PROCESSES INVESTIGATED	47
6.2 MANUFACTURING PROCESSES SELECTED	48
6.3 MANUFACTURING MILESTONES.....	50
7. TESTING PLAN	51
7.1 OBJECTIVES AND SCHEDULES.....	51
7.2 PROPULSION TESTING.....	52
7.3 INTEGRATION OF PRODUCTION AIRCRAFT INTO MANUFACTURING SUPPORT AIRCRAFT.....	53
7.4 STRUCTURAL TESTING.....	53
7.5 FLIGHT TESTING.....	54
7.6 CHECKLISTS.....	54
8. PERFORMANCE RESULTS	56
8.1 COMPONENT AND SUBSYSTEM PERFORMANCE	56
8.2 SYSTEM PERFORMANCE	57
9. REFERENCES	60



ACRONYMS AND NOMENCLATURE

C.G.	–	Center of Gravity	e	–	Oswald Efficiency
RAC	–	Rated Aircraft Cost	P	–	Power
TFS	–	Total Flight Score	S	–	Area
GS	–	Ground Score	Kv	–	Motor Voltage Constant (V)
EW	–	Empty Weight	K_D	–	Wing Loading Dissipative Constant
TMS	–	Total Mission Score	K_T	–	Thrust Loading Dissipative Constant
M1	–	Mission One	K_A	–	Regressive Constant
M2	–	Mission Two	\dot{x}	–	Position Derivative with respect to time
M3	–	Mission Three	V	–	Velocity
FOM	–	Figures of Merit	\dot{V}	–	Velocity Derivative with respect to time
FS	–	Flight Score	m	–	Mass
TOFL	–	Takeoff Field Length	T	–	Thrust
S_g	–	Takeoff Roll Distance	D	–	Drag
NiCad	–	Nickel-Cadmium	\bar{p}	–	Dimensionless Rolling Rate
NiMH	–	Nickel-Metal Hydride	\bar{q}	–	Dimensionless Pitching Rate
AVL	–	Athena Vortex-Lattice	\bar{r}	–	Dimensionless Yawing Rate
\tilde{C}_L	–	Airfoil Section Lift Coefficient	AR	–	Aspect Ratio
\tilde{C}_D	–	Airfoil Section Drag Coefficient	R_e	–	Reynolds Number
\tilde{C}_m	–	Airfoil Section Moment Coefficient	R_T	–	Taper Ratio
C_L	–	Aircraft Lift Coefficient	S_w	–	Wing Area (ft^2)
C_D	–	Aircraft Drag Coefficient	T_s	–	Settling Time (s)
C_f	–	Skin Friction Coefficient	ρ	–	Density
C_Y	–	Aircraft Side Force Coefficient	T_d	–	Doubling Time (s)
C_n	–	Aircraft Yawing Moment Coefficient	W	–	Weight (lbs)
C_m	–	Aircraft Pitching Moment Coefficient	α	–	Angle of Attack (degrees)
C_I	–	Aircraft Rolling Moment Coefficient	β	–	Sideslip Angle (degrees)
$C_{D,i}$	–	Aircraft Induced Drag Coefficient	μ_r	–	Rolling Coefficient of Friction
$C_{D,0}$	–	Aircraft Zero-Lift Drag Coefficient	R_{ls}	–	Wing Sweep
L'	–	Wing Thickness Location Parameter	R_{wf}	–	Wing Fuselage Interference
PA	–	Production Aircraft	MSA	–	Manufacturing Support Aircraft
MTOW	–	Maximum Takeoff Weight	V_{wind}	–	Wind Speed
Θ_{wind}	–	Wind Direction	$W_{battery}$	–	Battrey Weight



1. EXECUTIVE SUMMARY

This report details the design, testing, and manufacturing of the Georgia Institute of Technology *Buzzedryoshka* entry in the 2015-2016 AIAA Design/Build/Fly (DBF) competition. The system is made of two aircraft, a Manufacturing Support Aircraft (MSA) and a Production Aircraft (PA) designed to successfully complete the following four tasks:

1. Empty Flight of Manufacturing Support Aircraft
2. Delivery of the Production Aircraft Subassemblies
3. Timely Assembly of Production Aircraft
4. Loaded Flight of Production Aircraft

At the time of this writing, *Buzzedryoshka* has flown 31 times.

1.1 Design Process

Buzzedryoshka is designed for victory. This is achieved through the development of a robust system capable of flying all missions reliably with minimum Rated Aircraft Cost (RAC). The conceptual design of a winning system involved converting the mission requirements and scoring criteria into a list of design metrics that were used to decide the preliminary configuration of the aircraft. Trade studies on wing loading and power were performed using historical data and computer tools to estimate drag and lift. Battery and motor combinations were evaluated to achieve the required propulsion. Stability analysis was performed using a vortex lattice model to determine the size and placement of lifting surfaces. A detailed design with dimensions was created, then prototyped and flight tested to validate assumptions made during the design.

1.2 Key Mission Requirements and Design Features

A successful system design and score arise from the successful balance of key mission requirements. Specific design metrics were developed for each mission requirement and scoring element to maximize system performance and the overall competition score.

Empty Weight: The aircraft's empty weight is a significant driver of total score. Empty weight is the weight of the airframe and propulsion system. The entire aircraft was designed to be as minimalistic as possible without compromising the ability to complete all three flight missions. This was accomplished by judicious use of composite materials combined with a highly efficient built up structure, while simultaneously using the lightest possible motor and battery.

Battery Weight: The final flight score is inversely proportional to the battery weight squared. *Buzzedryoshka* was designed to require as little power as possible to complete all three flight missions. This was accomplished by minimizing drag and structural weight wherever possible.



Takeoff Requirement: The MSA and PA are required to takeoff in 100 feet on all missions. Fulfilling takeoff requirements requires a balance between wing area and propulsive power. This was accomplished with an aerodynamically efficient structure with minimal power required to fulfill the mission requirements.

Subassembly Requirement: The PA is required to fit within the MSA by breaking into multiple subassemblies. It is necessary to design the PA to have as few subassemblies as possible in order to maximize final score. The required number of subassemblies to maximize the final score is one. As a result, the PA was designed as one piece and the MSA was designed in multiple sections to fit around the PA.

1.3 Performance Capabilities of the System

All of the specific design features created to maximize the performance of the system can be summarized by the following performance capabilities:

- PA Max Takeoff Weight 3.39 lbs
- MSA Max Takeoff Weight 2.10 lbs
- Reliable takeoff within 100 feet
- Top speed of 35+ mph
- Single subassembly PA
- Multi-section design of MSA
- Secure storage of payloads in M2 and M3
- Proven capability through two iterations per aircraft and 31 test flights, as shown in Figure 1.1
- Estimated RAC of 0.96 and flight score of 18.73



Figure 1.1: Aircraft in flight.

The final design of the PA is a conventional high wing monoplane configuration with a single motor and tail-dragger gear. The aircraft is designed to simultaneously minimize weight and subassembly count, while maximizing speed. The canards, wings, fuselage and tail of the MSA are designed to assemble around the propeller, wings, fuselage and tail of the PA. The designs build on the teams' previous experience while continuing to push the envelope of practical, minimalistic design processes. The team is confident that this design solution has been optimized to accomplish all performance requirements and maximize total score.



2. MANAGEMENT SUMMARY

The *Buzzedryoshka* team consisted of twenty-six students: one graduate student, eight seniors, six juniors, three sophomores, and eight freshmen. Seventeen of the twenty-six students were returning members from the 2014-2015 Georgia Tech DBF entry. This team composition allows new team members to be mentored by a core of experienced members to build the team knowledge base and lay the foundation for later years.

2.1 Team Organization

Buzzedryoshka used a hierarchical structure to establish leadership amongst its senior members, with responsibilities flowing down to the team's newer members. This hierarchy served as an outline only, as all team members collaborated extensively to reach deadlines, share ideas, learn various disciplines, and produce a more successful aircraft. The work was divided during the design phase into CAD and Structures, Aerodynamics, Electrical and Propulsion, Payload, and Manufacturing. During construction, testing, and report writing, all team members participated fully. Figure 2.1 shows the different positions and the roles of each member of the team.

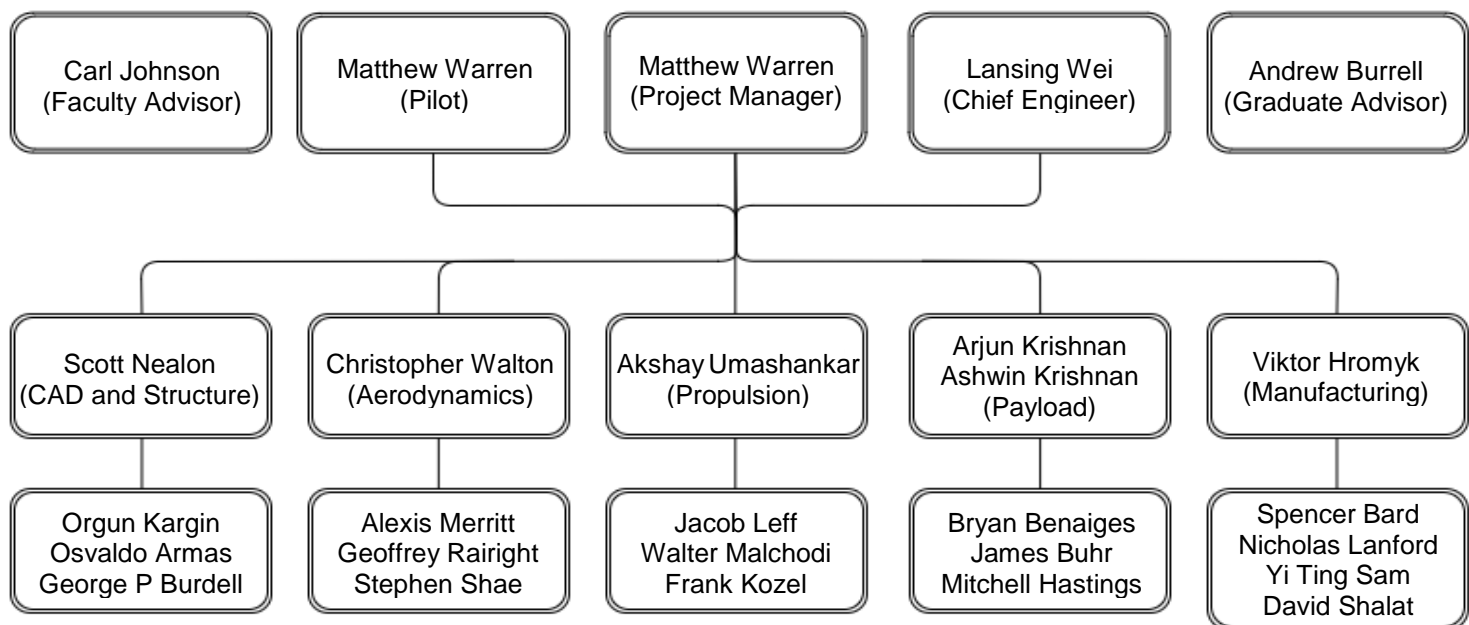


Figure 2.1: Team organization chart.



2.2 Milestone Chart

A milestone chart was established at the beginning of the design process to capture major deadlines and design and manufacturing goals. Progress was monitored by the team leaders to ensure all major milestones were met. The team worked throughout the entire academic year and established stringent deadlines early to ensure testing and flight experience before the competition in April. The team met frequently with the faculty advisors to discuss progress. The milestone chart is shown below in Figure 2.2, capturing planned and actual timing of major events.

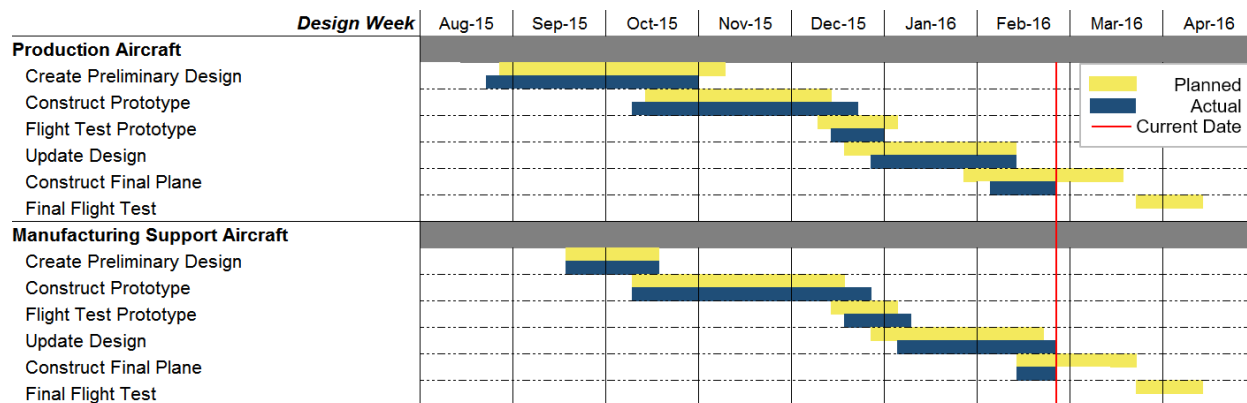


Figure 2.2: Aircraft design milestone chart showing planned and actual objectives.

3. CONCEPTUAL DESIGN

In this early phase of the design, the team analyzed the competition rules to produce a feasible design to maximize score. The rules were distilled into design requirements and scoring factors. Quantitative analysis was performed to pinpoint key scoring drivers and identify the design space. The scoring factors were translated into Figures of Merit (FOM) and used to weigh design choices. The FOM were applied to a design space of three possible system configurations to arrive at an optimized system. The PA is a high wing, conventional tail and single motor configuration that fits as a single piece into the MSA, which has similar configuration and assembles around the PA.

3.1 Mission Requirements

3.1.1 Mission and Score Summary

The AIAA Design/Build/Fly 2015/2016 competition consists of three flight missions, an optional ground mission, and a design report. The total score for each team is calculated as shown in Equation 3.1:

$$\text{Score} = \text{Written Report Score} \times (\text{TMS}/\text{RAC}) \quad (3.1)$$

Where TMS stands for the Total Mission Score made up of the two MSA missions (MF1, MF2), the PA mission (PF) and the optional bonus mission as shown in Equation 3.2:



$$TMS = MF1 \times MF2 \times PF + Bonus \quad (3.2)$$

Rated Aircraft Cost (RAC), is calculated from empty weight (EW) and battery weights ($W_{battery}$) of the two aircraft and the number of components ($N_{Components}$) used to construct the PA and is seen in Equation 3.3:

$$RAC = EW_1 \times W_{Battery,1} \times N_{Components} + EW_2 \times W_{Battery,2} \quad (3.3)$$

Equations 3.1 through 3.3 show that battery weights and number of components are the main score drivers, whereas various performance points of the design affect only the flight scores.

All flight missions are flown along the same distance and pattern per lap. For flight missions, the individual portions of the flight pattern seen in Figure 3.1 are as follows:

1. Successful Takeoff within 100 ft.
2. Climb to Safe Altitude
3. 180° U-turn, 500 ft. Upwind from the Start/Finish Line
4. 1000 ft. Downwind
5. 360° Turn Along the Backstretch
6. 180° U-turn
7. 500 ft. Final with a Successful Landing

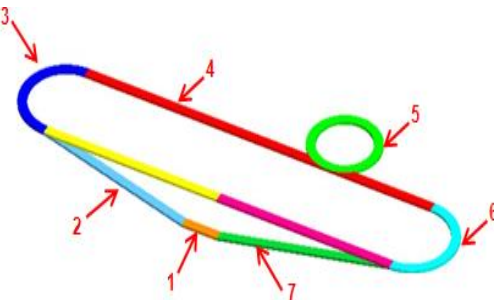


Figure 3.1: Competition flight course.

Each lap is roughly 2500 ft. when accounting for the three turns involved. A complete lap is defined as crossing the start/finish line, completing the defined pattern, then crossing the start/finish line while still in the air. The required number of laps is defined by the mission. The bonus mission will take place after the third flying mission and is driven by the assembly time. The full score is awarded as long as the PA is assembled within two minutes.

Mission 1 MSA Ferry Flight: The aircraft must take off within the designated field length and fly three laps within 5 minutes. Time starts when the aircraft is throttled up and a lap is complete when the aircraft passes the start/finish line. The score is awarded if the aircraft successfully completes the mission. The scoring for MF1 is shown in Table 3.1:

Table 3.1: Scoring Breakdown for Mission 1.

Mission	Description	Score
MF1	Aircraft completes the mission	2.0
MF1	Aircraft does not attempt or complete a successful flight	0.1



Mission 2 MSA delivery flight: This mission simulates the delivery of the PA and must be completed within a 10-minute window. The aircraft must take off in the designated field length, complete one lap carrying a sub assembly internally, return, and land successfully. A new subassembly is loaded and the plane is made ready to fly. The mission ends once every sub assembly has been successfully delivered. The scoring of MF2 is shown in Table 3.2:

Table 3.2: Scoring Breakdown for Mission 2.

Mission	Description	Score
MF2	Aircraft completes all sub-assembly group transport flights successfully within the time window	4.0
MF2	Aircraft completes less than all the sub-assembly flights within the designated time allowance but at least 1 group is successfully transported	1.0
MF2	Aircraft does not attempt or complete a successful flight	0.1

Mission 3: Production Aircraft Flight: The aircraft must take off in the designated field length. The payload for mission three, a factory sealed 32 oz. Gatorade bottle, must be carried internally. The aircraft must fly three laps within the five-minute time limit. Time starts when the aircraft is throttled up and a lap is complete when the aircraft passes the start/finish line. Landing is not included in the five min time limit. Listed in Table 3.3 below are the possible scores for mission three.

Table 3.3: Scoring Breakdown for Mission 3.

Mission	Description	Score
PF3	Aircraft completes the required flight within the time period carrying the full payload	2.0
PF3	Aircraft completes less than the required laps or exceeds the time period	1.0
PF3	Aircraft does not attempt or complete a successful flight	0.1

3.1.2 Aircraft Constraints

The competition rules stipulate specific constraints on the aircraft's takeoff distance, propulsion system, and payload:

Takeoff Distance: The aircraft must have the ability to start and take off completely within a 100 foot runway for all three flight missions.



Propulsion System: The aircraft must be propeller driven and electrically powered, with all components of the propulsion system commercially available. These include the motor, propeller, speed controllers, receivers, and batteries. The battery selection is limited to NiCad or NiMH, but may be of any cell count, voltage, or capacity. There is no limit of the weight of the battery packs. The entire propulsion system must be armed by an external safety plug or fuse. The arming device must be mounted on the exterior of the aircraft and be accessible from behind in a tractor propeller configuration.

Payload: The payload for the PA is a full, factory sealed 32 oz. Gatorade bottle. The MSA payload is the PA broken down into subassemblies. All payloads must be secured within the aircraft's structure so that they do not shift or come loose during flight.

3.1.3 Flight Score Sensitivity Analysis

A sensitivity analysis on the flight scoring drivers was performed to understand the design trades and mission objectives that maximize the total mission score (TMS) as divided by the rated aircraft cost (RAC). It is assumed that the system can complete the missions if the respective flight speeds exceeds the minimum speed and meets the takeoff requirement with payload. The scoring then becomes a function of RAC alone, which is driven by the number of components of the PA, battery weights, and structural weights.

Component count: The flight score is inversely proportional to the number of components of the PA. The effect of Number of components was studied by applying constraints to the scoring equation. The battery weight was estimated at 40% of the system empty weight for both aircraft, and payload fraction for the PA was estimated at 0.65 from historical data. This allowed the RAC to be expressed as a function of MSA empty weight and number of PA components. Final Score was then plotted against empty weight, with both axes being expressed as percentages of baseline values. This is shown in below in Figure 3.2.

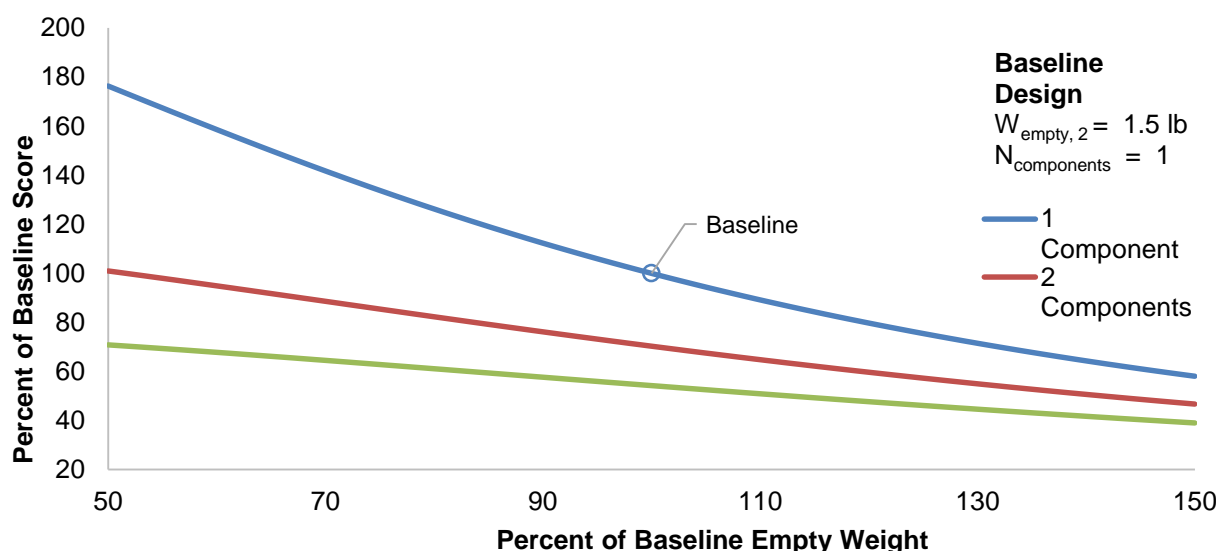


Figure 3.2: Change of score with respect to empty weight and number of components.



As seen in the figure, empty weight of the MSA would need to be reduced by 50% to justify the increase from 1 to 2 components. Achieving a competitive Final Score demands a single-component PA design.

Empty Weight: Aircraft empty weight was divided into propulsion and structural components. The propulsion system weight is proportional to the number of battery cells used. Based on previous team experience, 1,500 mAh NiMH cells were selected as representative batteries, weighing 0.05 lbs each. Based on testing of battery discharge rate, the maximum current draw is 20 amps. The electric motor weight was estimated at 0.5 lbs / kW from past experience, and speed controllers that met the pack voltage were cataloged. The propulsion weight assessment is summarized by Equation 3.4 and Equation 3.5:

$$P_{electric} = n_{cells} \left(1.2 \frac{V}{cell} \times 20 \text{amps} \right) \quad (3.4)$$

$$W_{propulsion} = n_{cells} \left(0.05 \frac{\text{lbs}}{cell} \right) + P_{electric} \left(0.5 \frac{\text{lbs}}{\text{kW}} \right) + W_{ESC} \quad (3.5)$$

Structural weight was estimated using the team's experience, with a baseline minimum weight which increases with wing area. The coefficients K_A and K_B in Equation 3.6 were adjusted to match past years' Design/Build/Fly planes, and Equation 3.7 summarizes the empty weight assessment:

$$W_{struct} = W_{baseline} + K_A (S_{wing} - S_{baseline})^{K_B} \quad (3.6)$$

$$EW = W_{struct} + W_{propulsion} \quad (3.7)$$

Maximum Speed: The MSA and PA need to be able to fly above 35 mph to complete three 2,500 ft. lap lengths within five minutes with the assumed wind conditions. The maximum speed was calculated using simple power-required calculations that stem from the drag polar, and the power available from the propulsion system, as seen in Equation 3.8. Lap numbers were truncated down, since only integer numbers of laps are counted.

$$P_{req} - P_{av} = \left(\frac{1}{2} \rho V_{max}^3 S C_{D,0} + \frac{2W}{\rho V_{max} S \pi A Re} \right) - P_{electric} \eta_{prop} = 0 \quad (3.8)$$

Takeoff: Both aircraft must be able to take off within 100 ft. on all missions. This requirement constrains the wing area and power requirement. The governing relation for takeoff is shown in Equation 3.9. The K_D term is a function of dissipative forces and wing loading (W/S), while K_T is a function of propulsive forces and thrust loading (T/W).

$$S_g = \frac{1}{2gK_D} + \ln \left(1 + \frac{K_D}{K_T} V_{LO}^2 \right) \leq 100 \text{ feet} \quad (3.9)$$

Since the sizing and payload is driven by the PA, analysis of the MSA follows the PA analysis. As a result, the scoring sensitivity in Figure 3.3 below only shows the RAC for the PA. The plot represents a physics-based tradeoff between speed and aircraft weight, as governed by wing area and battery count. The white area represents configurations that cannot meet the takeoff and speed requirements.

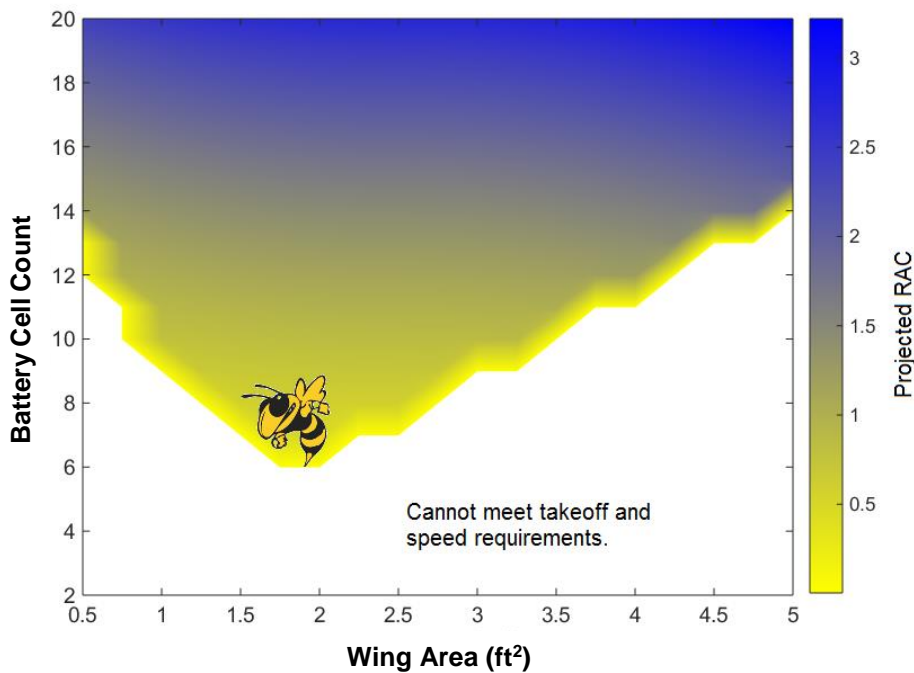


Figure 3.3: A physics-based scoring analysis of the design space for the PA. The team's chosen conceptual design point is noted by Buzz.

The figure demonstrates that the design with the highest scoring-potential which can successfully complete the mission, must have the lowest possible cell count. This corresponds to a 7 cell battery and a wing area of about 1.8 sq. ft. This was the conceptual design point for the PA.

A similar analysis was completed for the MSA. The wing area for the MSA is constrained to be about 50% larger than the PA to internally accommodate the wings of the PA. The estimated payload of the MSA is found from the preliminary analysis of the PA. With wing area fixed at a minimum and payload known, it was only necessary to compute the smallest battery that could meet the mission requirements.

3.1.4 Ground Score Sensitivity Analysis

The bonus mission does not present any aerodynamic trade-offs and must be analyzed separately from the flight missions. Since the PA must be one piece, the assembly time should be short. Due to the pass-fail nature of the bonus mission, it is only necessary to design the PA in a way that allows it to be assembled with payload in just under the required time of 2 minutes.



3.2 Translation into Design Requirements

The scoring analysis revealed four main components that drive the overall flight score:

Component Count: Any component on the PA that is disconnected or moved from its position required for takeoff and flight will be counted as a sub-assembly. Additionally, landing gear that is retracted or removed to fit inside the MSA or a propeller that folds or is removed will count as a sub-assembly. For the maximum achievable score, the component count needs to be the absolute minimum. This suggests a single piece PA with no components removed to fit inside the MSA.

Empty Weight: Any configuration that fails to be as light as possible will not be competitive. Effort must be made to reduce the aircraft empty weight. However, the structure must be able to withstand the expected loads. Such considerations must be carefully balanced to secure the payload and decrease empty weight.

Battery Weights: Larger batteries provide more power and will enable faster flight. However, larger batteries also incur a larger weight penalty. Based on analysis of the scoring, the battery weights will have the largest individual impact and must therefore be optimized to provide the power required without adding unnecessary weight.

Flight Speed: The aircraft must be able to fly the required number of laps in Wichita, Kansas. Figure 3.4 shows a distribution of mean wind speeds in Wichita, Kansas over the past 10 years in April. It is unreasonable to design for the maximum recorded speed so a 97% confidence interval was chosen. The mean wind speed on the day of the competition will be less than about 25 mph with 97% certainty.

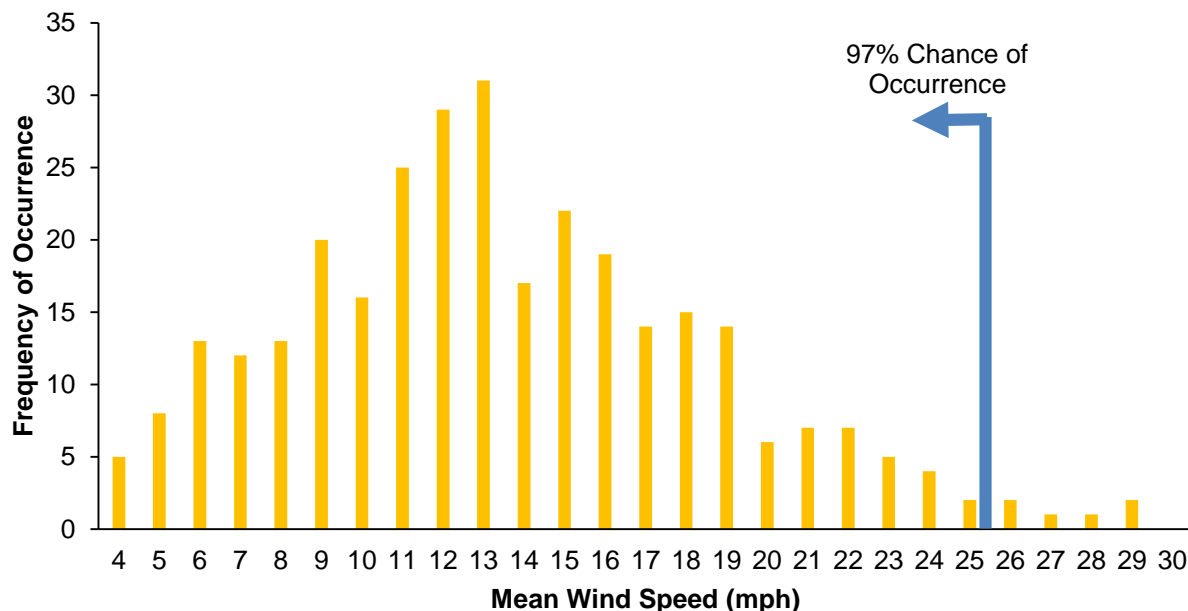


Figure 3.4: Distribution of mean wind speeds in Wichita, Kansas in April.



Any given wind speed corresponds to a required flight speed to finish the missions. This required speed is assumed the plane must travel 1000 ft upwind per lap and 1500 ft downwind per lap. It can be seen in Figure 3.5 that a wind speed of 25 mph translates to an aircraft flight speed of under 35 mph. A minimum flight speed of 35 mph was chosen as a minimum speed for both the PA and the MSA.

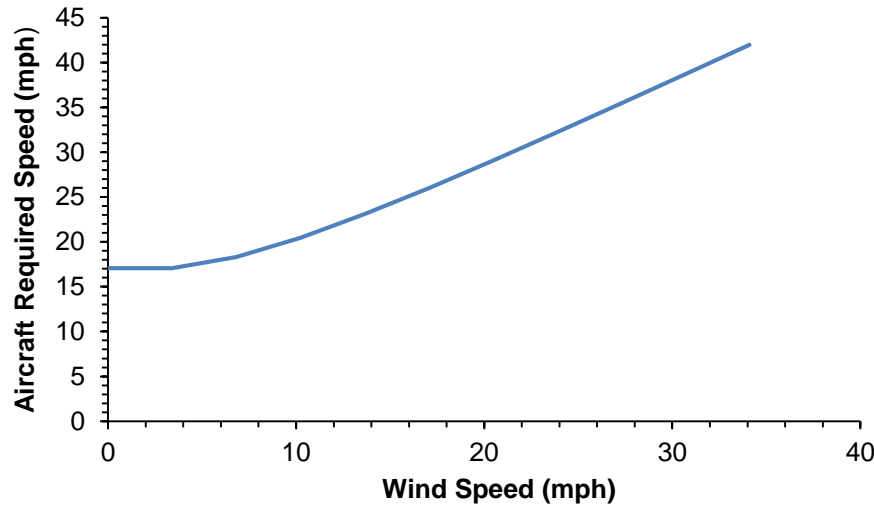


Figure 3.5: Required top speed to complete Mission 3 versus wind speed.

The analysis conducted in Sections 3.1 and 3.2 were translated into qualitative design metrics that were used to evaluate and select an aircraft configuration, summarized for the PA and MSA in Table 3.4 below.

Table 3.4: Rules and requirements translated into design requirements.

Mission/Scoring Requirement	Design Requirement
Minimal Component Count	Simple, Robust Design
Low Empty Weight	Efficient Structure
Minimal Battery Weight	Optimized Propulsion
Enclose Production Aircraft	Unique geometry
	Robust, multi-part Design

These requirements show that minimizing the number of components for the PA is the most critical design consideration, followed closely by battery weights. If a design is as light as possible, it will also likely require less power and have the lowest battery weight. The MSA must fit tightly around the PA to be efficient, indicating that it must have the same configuration.



3.3 Configurations Considered

3.3.1 Aircraft Configuration

Due to the nature of the competition rules, both aircraft had to be developed simultaneously as a system. Since the planes need to nest together, the selection criteria hinged on the complexity of wrapping the MSA around the PA. As a result, several design possibilities are eliminated, but three choices emerged as possible configurations. Each of these configurations were thoroughly analyzed, as detailed below.

In Figure 3.6 through Figure 3.8, the wire frame represents the MSA while the shaded figure represents the PA. Figure 3.6 shows a basic biplane configuration for both the PA and MSA. With a biplane, the MSA would require two removable wings and a two-part, bulbous fuselage to allow the PA to fit inside as a single piece with landing gear. This complexity would present a significant structural challenge and likely increase the weight of the plane. These drawbacks would make this configuration a difficult choice.

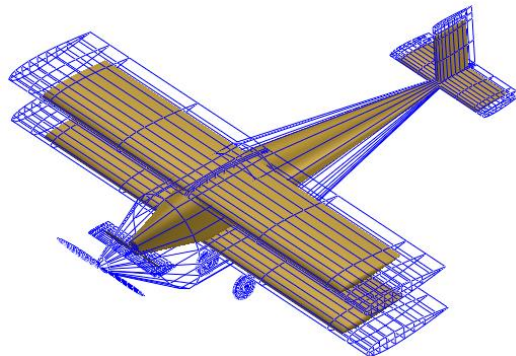


Figure 3.6: Sketch of biplane configuration.

A flying wing configuration was examined, shown in Figure 3.7. In this case, the MSA would need to have a large opening or be built in two halves to allow the PA to be loaded. The MSA would also require a fuselage bottle fairing, and landing gear of the PA leading to structural complexity. In addition, a flying wing is sensitive to C.G. and has a high power requirement due to a low $C_{L,\max}$.

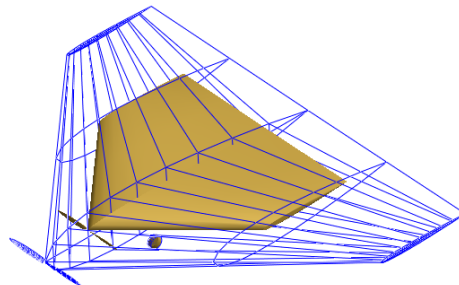


Figure 3.7: Sketch of Flying Wing configuration.



Finally, the team explored a conventional monoplane configuration, illustrated in Figure 3.8. This configuration would still require the wings of the MSA to be detachable and have some method to enclose the PA propeller. However, the fuselage would only require a hatch to accept the PA. Moreover, this configuration would allow for minimization of interference from the PA landing gear and payload bay. As a result, the conventional configuration should be lighter than the biplane and more stable than the flying wing, making it qualitatively superior.

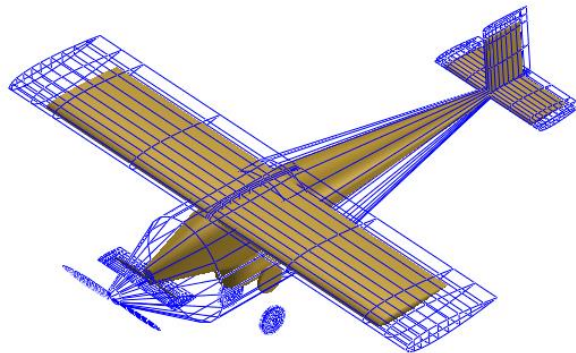


Figure 3.8: Sketches of Conventional configuration.

3.4 Component Weighting and Selection Process

In order to asses each configuration from a quantitative standpoint, Figures of Merit (FOM) were created based on the most important configuration factors. The FOM are shown in Table 3.5. Each FOM was assigned an importance of 0 through 5, with 5 being the most important factor and 0 being a non-factor in design.

Table 3.5: Figures of Merit.

Figure of Merit	0	1	2	3	4	5
Simplicity						5
Weight					4	
Power				3		
Speed				3		
Stability			2			
Drag			2			

All of the configurations could be made with a minimal number of components. As such, the simplicity of enclosing the PA inside of the MSA was the critical design factor. Due to the wind conditions anticipated at the location for this year's competition, Wichita KS, speed was another consideration. Minimizing both weight and the power requirement maximizes flight score and makes them important score drivers.

For final selection, each configuration was given a scoring value for each figure of merit, and that rating was then multiplied by the FOM value. The range of scoring values are shown in Table 3.6. The configuration with the highest total quality was then selected for further analysis in the design process.



Table 3.6: Configuration Scoring Values.

Score	Value
1	Inferior
3	Average
5	Superior

The three configurations discussed previously are shown in Table 3.7 with their respective scores for each of the relevant FOM. These results, combined with those from the qualitative analysis, lead to the team's choice of configuration for the *Buzzedryoshka* aircraft system.

Table 3.7: Aircraft configuration Figure of Merit.

Aircraft Configurations				
FOM	Value	Conventional	Flying Wing	Biplane
Simplicity	5	3	2	1
Weight	4	4	1	2
Power	3	4	2	4
Speed	3	4	5	3
Stability	2	4	2	4
Drag	2	4	2	2
Value	19	71	43	46

The complexity of the biplane and power requirement of the flying wing made these designs ill-suited for the PA. The conventional monoplane configuration had the highest total score, and was therefore chosen as the configuration for both aircraft in the combined system.

3.5 Final Conceptual Design Configuration

The final configuration for both the PA and MSA is a high wing, conventional tail aircraft with a single-engine tractor propulsion system as shown in Figure 3.9. Here the MSA is shown exploded into several pieces to show how the PA will fit within. This configuration offers minimal complexity for nesting, while allowing for greater speed by reducing drag. The empty weight of the aircraft is more heavily influenced by structural design, and is discussed later in this report.

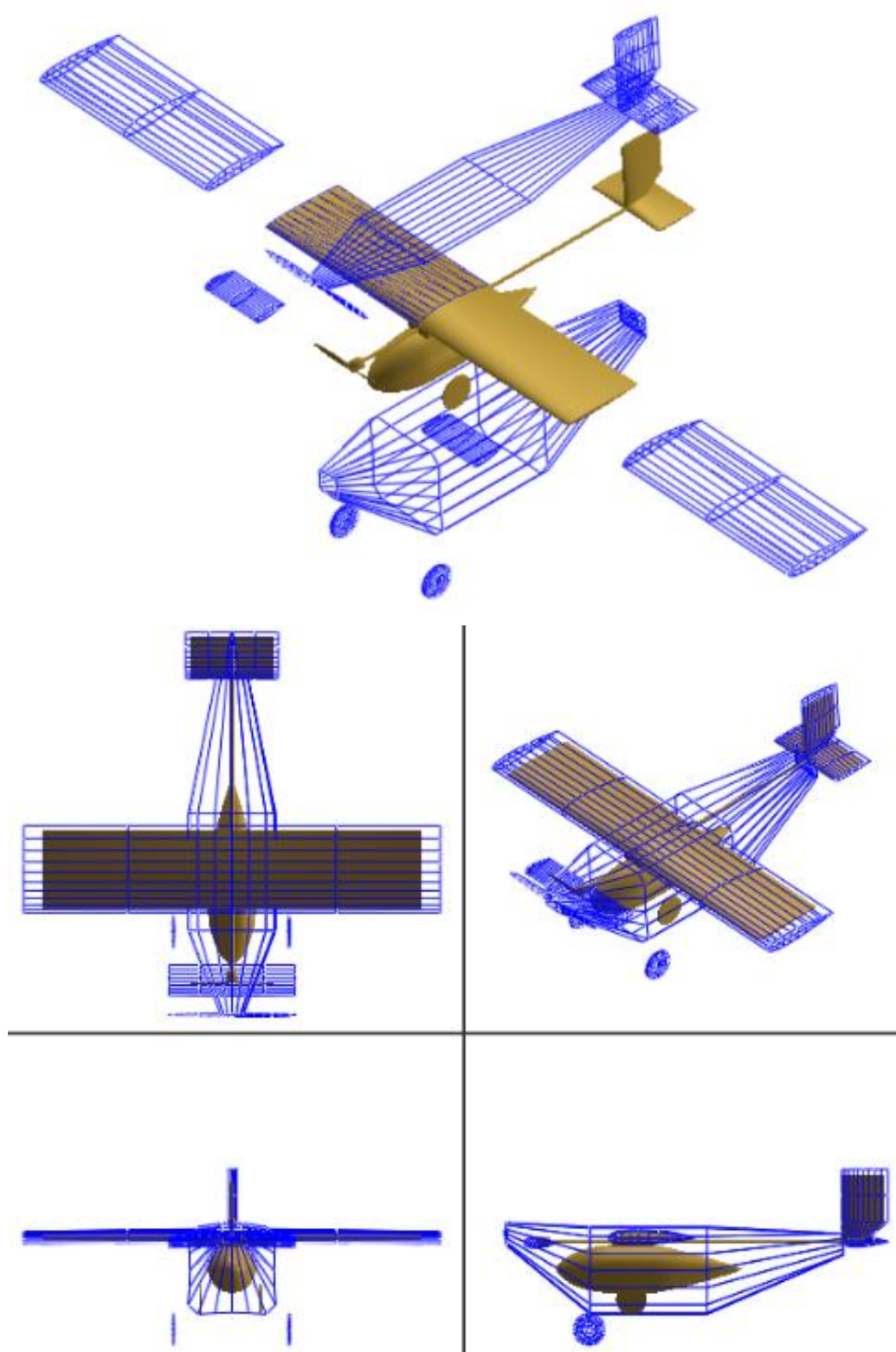


Figure 3.9: Final Configuration.



4. PRELIMINARY DESIGN

The objective of the preliminary design phase was to further narrow the design space. To do this, design/sizing trades for the system were evaluated by examining propulsion system options and wing area sizing for takeoff distance. The weight, drag, motor, propeller data, battery data, and aerodynamic coefficients were calculated and combined to estimate mission performance for all three flight missions.

4.1 Design Methodology

The *Buzzedryoshka* team designed the two aircraft configurations in parallel using an iterative performance-focused multidisciplinary analysis. The team used constraint sizing to select a weight-normalized design point for each plane that could satisfy objectives for all three missions. From these design points, the team analyzed possible propulsion systems, aerodynamic characteristics, built mission models, and compared them to estimates generated as part of the sizing process. After this analysis, the mission performance and stability of the sized aircraft configurations were computed. The design process detailed in sections below is written as sequential, but iterations occurred throughout, as seen in Figure 4.1. An example of iteration would be updating wing area at a constant wing-loading if propulsion weight is found to be lower, re-evaluating stability and mission performance, and re-adjusting the wing or propulsion system if needed. All iterations were performed with the ultimate goal of maximizing overall score. Therefore, the design shown in this report is the final product of a more complex, iterative procedure.

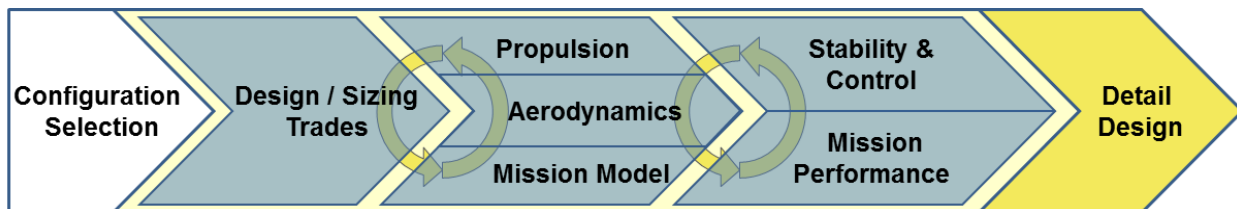


Figure 4.1: The team's preliminary design methodology highlighting multidisciplinary iterations.

4.2 Design Trades

4.2.1 Constraint Sizing

A constraint sizing analysis was conducted to examine the effect of wing loading and power to weight ratio on the performance and scoring potential of each aircraft. The MSA must be designed after the PA to ensure the MSA can carry the PA. As specified in Section 3.1.3, the scoring requires the planes to finish the missions while having a minimal battery weight. Figure 4.2 shows the relationship between wing loading (W/S) and power to weight (P/W) for the PA.

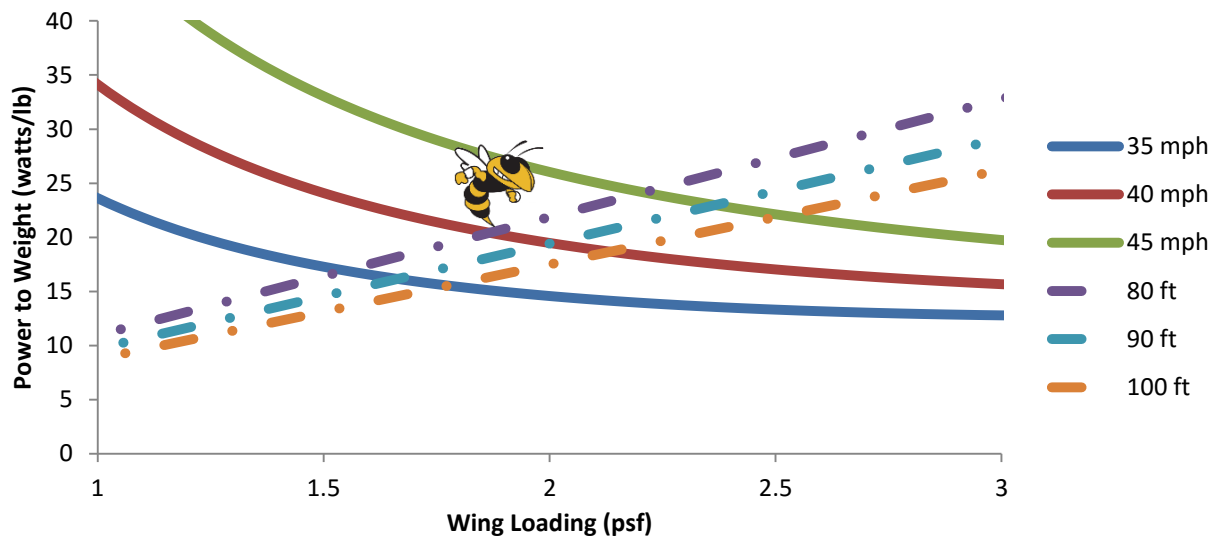


Figure 4.2: Design point of the PA from the constraint plot, marked by Buzz's stinger.

Battery weight is roughly proportional to power available, and the lowest P/W possible will lead to the highest score. Higher W/S allows for lower P/W required at cruise, but higher P/W to meet takeoff requirements. The inverse is also true. The optimal design is at the intersection of the required takeoff distance and minimum speed required. Based on these considerations, a design point just above the 80 ft. takeoff distance and with a top speed just above 40 mph was chosen.

The wing area of the MSA was constrained by its need to closely fit the PA and carry it in Mission 2, creating a fixed minimum W/S of 0.7. Since minimum wing area corresponds to minimum weight, this W/S was used and the propulsion system sized to match, as shown in Figure 4.3 below.

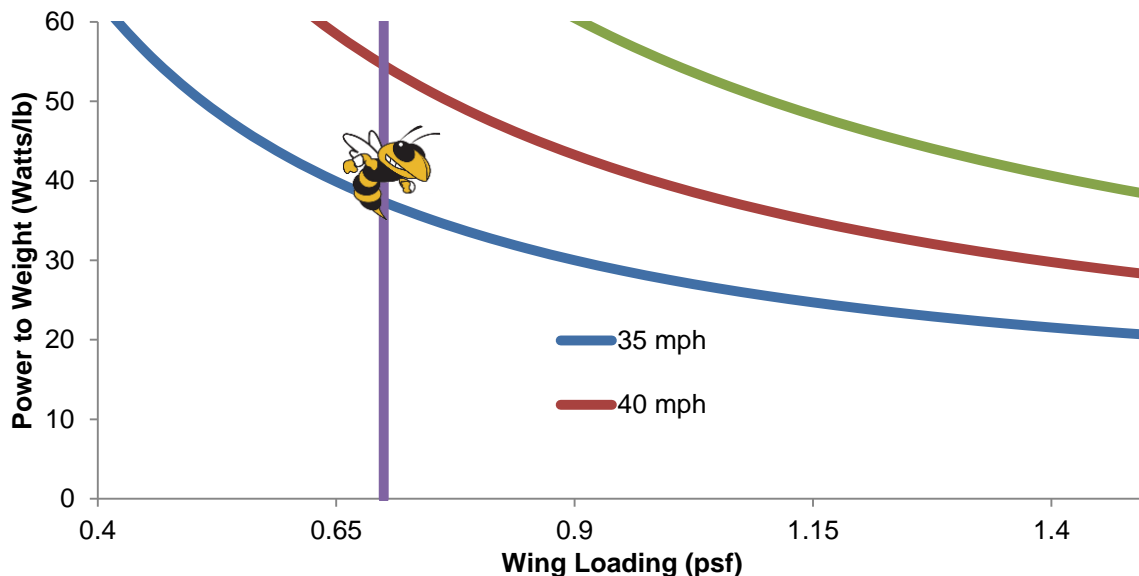


Figure 4.3: Design point of the MSA from the constraint plot, marked by Buzz's stinger.



Note that takeoff curves are not shown in the figure. This is because analysis showed that the P/W required for takeoff was much smaller than that for cruise at higher the speeds shown in the figure. This meant P/W for cruise speed dominated the constraint sizing analysis for the MSA. The final design point for the MSA achieves a cruise speed of just over 35 mph.

The constraint sizing process along with an empirical weight estimate allow a preliminary determination of power and wing area summarized in Table 4.1 for the PA and MSA.

Table 4.1: Preliminary Power and Wing Area.

	Wing loading (psf)	Power Loading (Watts/lb)	Est. Weight (lb)	Surface Area (Sq. ft)	Power Req. (Watt)
Production	1.81	21	3.4	1.875	71.4
Manufacturing	0.71	37	2.1	2.87	77.7

4.2.2 Propulsion System Selection

As seen in Table 4.1, the power requirement for each aircraft is similar. As a consequence, the same propulsion system will be used for both aircraft. The team decided to use a fixed pitch propeller because of reduced complexity and weight. A system efficiency of 50% is empirically assumed leading to a power of around 160 watts for the propulsion system. From the analysis performed in section 3.1.3, a 7-cell 1500mAh battery maximizes RAC. The team wanted a direct-drive brushless out-runner motor with a high motor constant, Kv, to draw more power out of a 7-Cell battery. The team researched motors that fit these criteria and created a database containing over 50 motors from various companies, including Hacker, Tiger, Scorpion, Cobra and AXI.

A propeller database was also generated based on the size of the airplane and speed. The propellers tested were APC 9x9, 10x7, 11x8, 12x8, and 12x10 propellers. MotoCalc, a commercially available motor analysis tool, was then used to estimate the motor efficiency, static thrust, and thrust at 30 mph for each motor and propeller combinations, feasible combinations were selected for further analysis and sorted by weight.

The top motor-battery-propeller combinations were analyzed and their variation with speed was graphed. Allowing the team to evaluate the most effective combination to meet the takeoff and max speed requirement. Two motor combinations were chosen to purchase and test, as shown in Table 4.2. Section 7.2 will go into further detail regarding these tests.

Table 4.2: Final propulsion alternatives.

Motor	Kv	Battery (Cells)	Current (Amps)	Best Propeller	Static Thrust (lb.)	Propulsion System Weight (lb.)
Cobra 2814/12	1390	7 (1,500 mAh)	19.0	12x8	1.89	0.15
Hacker A30- 22S	1440	7 (1,500 mAh)	17.0	11x8	1.37	0.24



4.3 Mission Model

4.3.1 Description and Capabilities

The three missions were simulated via a set of first order differential equations (Equations 4.1-4.3) defining the position and orientation of the vehicle throughout the flight. By integrating these equations over time using a 4th Order Runge-Kutta approach in MATLAB and simple logic defining each of the required mission segments, it is possible to define the position, velocity, and orientation of the vehicle over time. The thrust (T) was defined as a function of velocity, with the relationship defined by MotoCalc, the analysis tool used in the propulsion system selection. The drag (D) was represented via a parabolic drag relationship. The load factor was explicitly defined for each turn segment, but if it exceeded the estimated maximum lift coefficient, it was limited to that value.

$$\dot{x} = V \quad (4.1)$$

$$\dot{V} = \frac{T - D}{m} \quad (4.2)$$

$$\dot{\psi} = \frac{g\sqrt{n^2 - 1}}{V} \quad (4.3)$$

4.3.2 Uncertainties

The approach described above has specific limitations and uncertainties. The lack of a vertical dimension means that it cannot capture any aerodynamic effect due to altitude changes, or for the energy required or saved due to climbing or diving. The lack of any wind model discounts any additional drag due to sideslip in flight, or changes in velocity depending on traveling with or against the wind. The flight path defined for each lap assumes an idealized flight path, with the pilot turning perfectly after each 1000 ft. leg and the turns being optimal turns. Finally, there are additional uncertainties in the mission predictions due to any errors or inaccuracies in the thrust and drag predictions.

4.4 Aerodynamic Characteristics

4.4.1 Airfoil Selection

Using the correct airfoil for the aircraft is key to achieve the aerodynamic characteristics required to compete in this competition. Hundreds of airfoils were analyzed through a MATLAB script at an estimated Reynolds number of 200,000 to choose an airfoil that could provide the requisite lift and moment coefficients. These airfoils were also filtered based on their thickness and manufacturability.



Manufacturability: Complex airfoil geometry, as shown in Figure 4.4, can result in manufacturing error. These imperfections can negatively impact the aerodynamics of the vehicle and therefore its performance. The airfoil must not have a highly cambered or sharp trailing edge while maintaining sufficient thickness to reduce these manufacturing difficulties and obtain the desired performance from an airfoil.

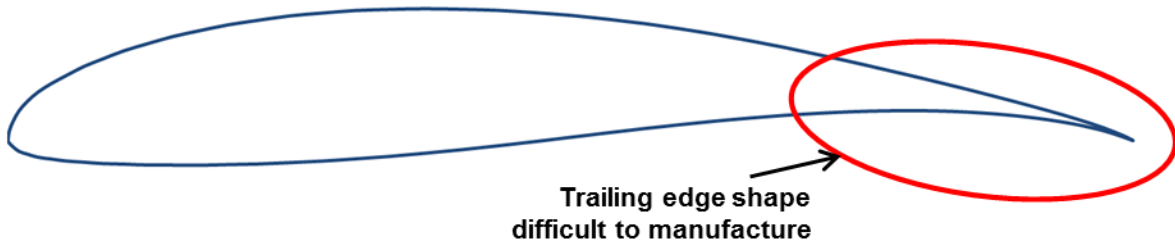


Figure 4.4: Wortmann FX 63-137 showing poor manufacturability.

Thickness: Low thickness airfoils typically have a small leading edge radius that results in abrupt stall at lower angles of attack. Increasing airfoil thickness increases the space for internal structural members that increase the structural rigidity of the airfoil while reducing structural weight. However, this trades with this year's requirement for nesting wings. After testing multiple airfoil types, a thickness greater than 12% was preferred for the MSA to achieve required structural rigidity and allow for nesting wings.

The filtered airfoils were further analyzed based on maximum section lift coefficient and lift to drag ratio. Drag and lift curves for the final four airfoils were constructed using airfoil data obtained from wind tunnel test results from UIUC as shown in Figure 4.5.

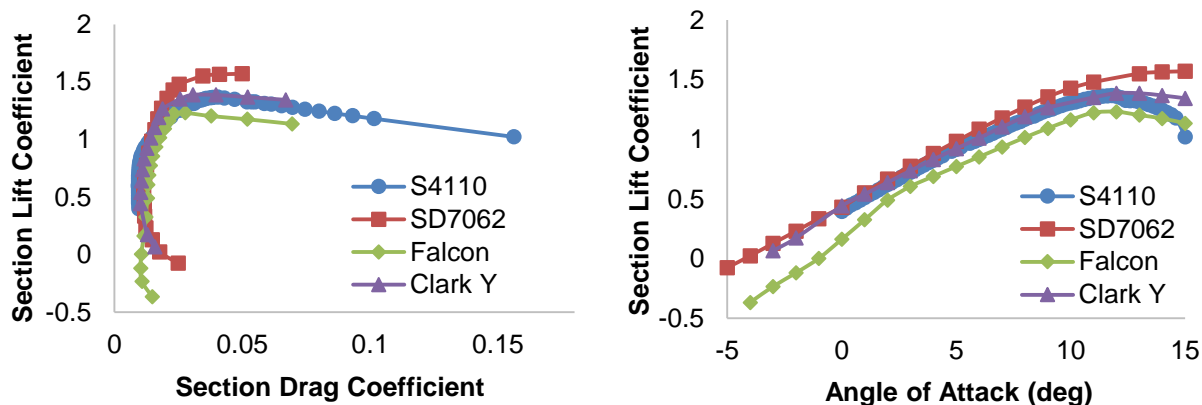


Figure 4.5: Experimental lift and drag characteristics for selected airfoils from UIUC data.

Examination of the drag polar shows that the SD7062 and S4110 airfoils have a more stable sectional drag coefficient (\tilde{C}_D) over longer ranges of \tilde{C}_L than the other airfoils. This indicates that for a given range of \tilde{C}_L values, namely those around a \tilde{C}_L of 0.5, the \tilde{C}_D remains relatively low and constant. This is important due to the variance of \tilde{C}_L over the wings caused by downwash due to wingtip vortices and environmental variables such as local wind. A high maximum \tilde{C}_L is a desirable airfoil characteristic as it enables good STOL performance, which is critical due to the 100-foot takeoff requirement.



The SD7062 has a thickness to chord ratio of 14% which aids in both the manufacturing process and increases the geometric stiffness of the wing. The SD7062 also had a higher maximum \bar{C}_L and lift-to-drag ratio than the other airfoils considered, enabling the team to select the best combination of takeoff performance and speed. In summary, the SD7062 airfoil was selected for its combination of high maximum \bar{C}_L , manufacturability, thickness to chord ratio, and favorable lift to drag ratio.

The S4110 is a thinner airfoil chosen for the PA based on its high maximum C_L , and relatively high lift to drag ratio. While the Clark Y airfoil has comparable performance, the lower thickness presents an advantage at the system level. Although the slender profile will impact the stiffness of the wing, this airfoil will not present any unreasonable manufacturing challenges. The integration of the S4110 airfoil into the SD7062 airfoil is shown in Figure 4.6 below.



Figure 4.6: S4110 inside of SD7062 airfoil.

4.4.2 Lifting Surface Analysis

Athena Vortex Lattice (AVL), an aerodynamic tool developed by Dr. Mark Drela at MIT, was used to model the lifting surfaces of the aircraft to compute the aerodynamic characteristics of the entire aircraft. AVL models lifting surfaces as an infinitely thin sheet of discrete vortices, and models their interactions. The aircraft's tail and control surfaces were sized in AVL to provide desired static stability and trim characteristics. The aircraft configuration and paneling in AVL is seen in Figure 4.7. The lift distribution shown in Figure 4.8 was generated in AVL using elevator trim to maintain flight at a moderate angle of attack on approach and landing. Due to the distribution shape, stall is expected to occur at the wing root, allowing the pilot to maintain roll control using the ailerons that are mounted outboard.

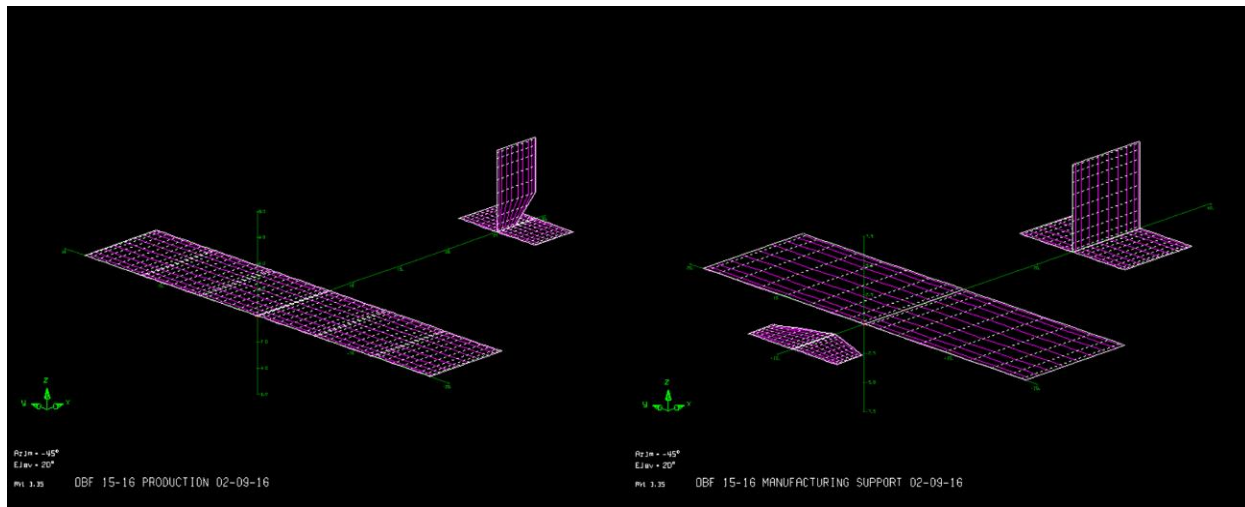


Figure 4.7: AVL model of both aircraft.

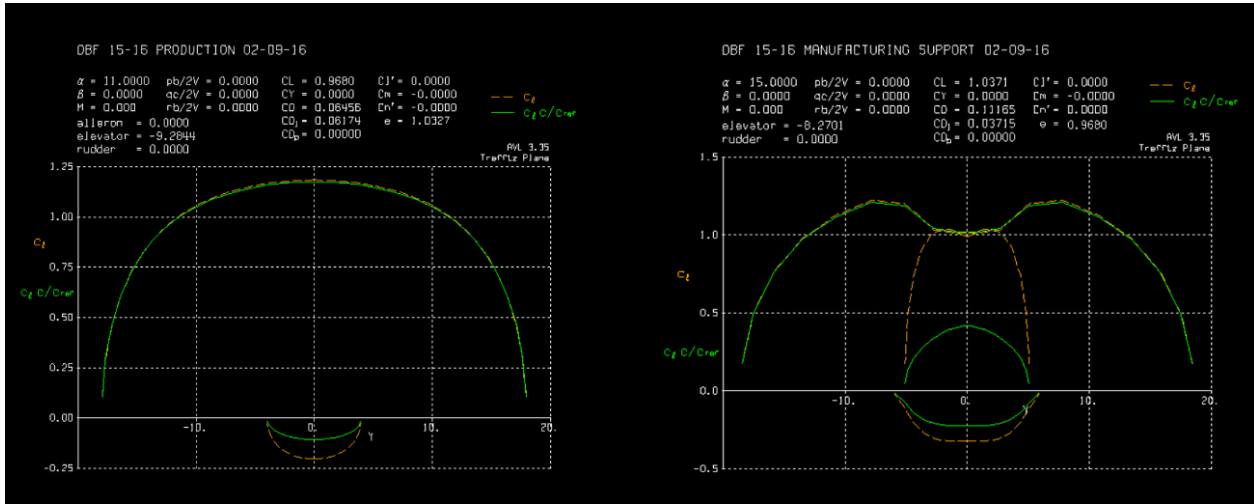


Figure 4.8: AVL predicted lift distribution of both aircraft.

4.4.3 Drag Analysis

A preliminary parasitic drag estimate was obtained by summing each component's drag contributions, computed using the semi-empirical methods from Hoerner's *Fluid Dynamic Drag*, and then normalizing each component according to the wing reference area. Table 4.3 shows the contributions of the major aircraft components, with displaying Figure 4.9 the same data as a percentage breakdown.



Table 4.3: Aircraft zero lift drag estimates.

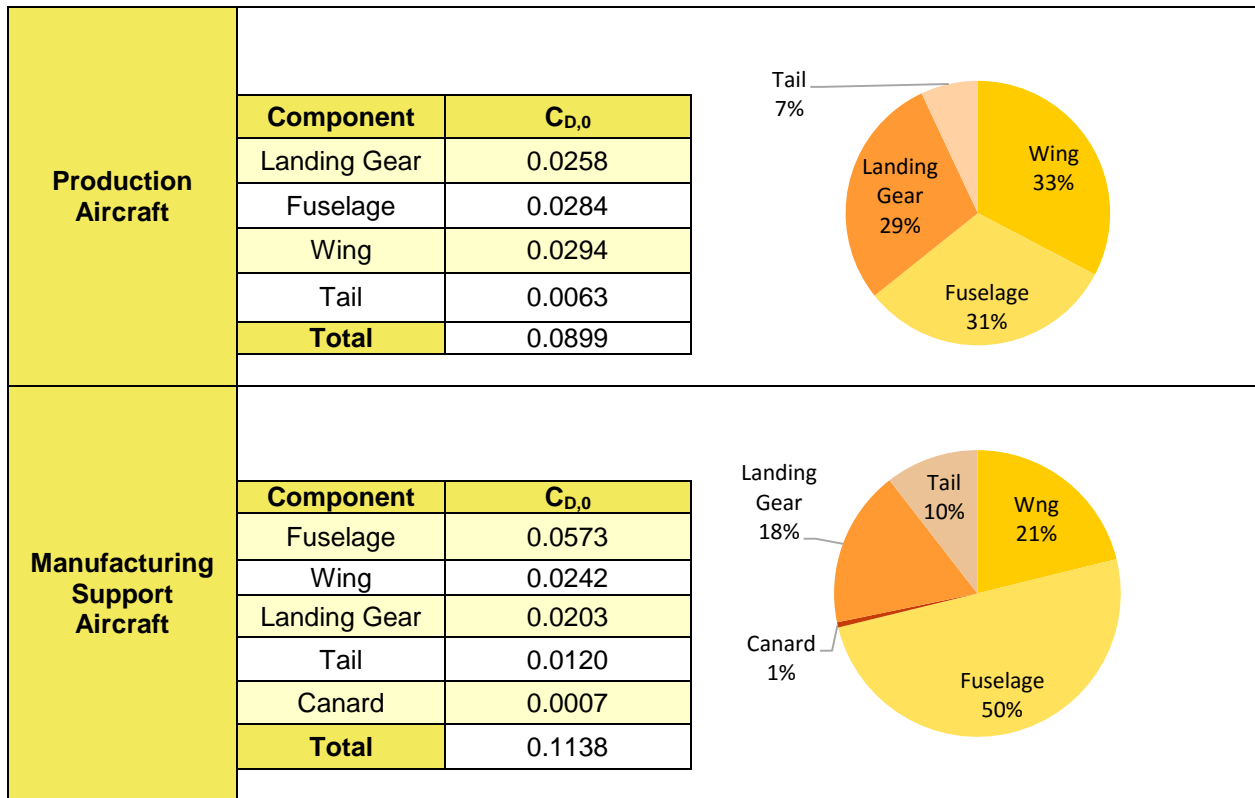


Figure 4.9: Graphical representation of drag estimates.

The main components of the parasitic drag are detailed below:

Wing: The drag coefficient for the wing was calculated using Equation 4.4 from Hoerner:

$$C_{D,0} = R_{wf} R_{LS} C_{f_w} \left(1 + L' \left(\frac{t}{c} \right) + 100 \left(\frac{t}{c} \right)^4 \right) \times \frac{S_{wet_w}}{S} \quad (4.4)$$

Equation 4.4 contains terms correcting for wing thickness location, sweep, and wing-fuselage interference (L' , R_{LS} , and R_{wf} , respectively). The flat-plate skin friction coefficient (C_f) is a function of Reynolds number approximated for fully turbulent flow. The wing was found to be the largest contributor to zero-lift drag for the PA, with a total $C_{D,0}$ contribution of 0.0258, which is about 33% of the total drag. For the MSA, the wing was found to be the second largest contributor to zero-lift drag, with a total $C_{D,0}$ contribution of 0.0242, which is about 21% of the total drag.

Landing Gear: The landing gear components are significant contributors to the overall drag of the aircraft. The main gear and tail gear drag contributions were calculated separately, but both were modeled as a wheel and a flat plate added for the strut. The overall contribution of the landing gear to the drag was about 29% for the PA and 18% for the MSA.



Fuselage: The drag coefficient for the fuselage was determined using Hoerner's method, which computes drag as a function of the body fineness ratio, the Reynold-adjusted skin friction coefficient, and lifting-surface/fuselage interference. The total $C_{D,0}$ contribution fuselage of the MSA was calculated to be 0.0573 and contributes 50% of the total zero-lift drag. The total $C_{D,0}$ contribution fuselage of the PA was calculated to be 0.0284 and contributes 31% of the total zero-lift drag.

Tail: The tail surfaces were modeled as wings and the drag contributions were calculated using the same method as the wing calculation. Overall, the contribution of the tail to the drag were 7% and 11% for the PA and the MSA, respectively, due to their small size.

Canard: The drag coefficient for the MSA canard was calculated using Equation 4.4 from Hoerner. The flat-plate skin friction coefficient (C_f) is a function of Reynolds number approximated for fully turbulent flow. Due to its small size, the canard was found to be one of the smallest contributors to zero-lift drag, with a total $C_{D,0}$ contribution of 0.0007. This is about 1% of the total drag.

With parasitic drag computed for both aircraft, the team used AVL to model the lifting surfaces of the aircraft and estimate induced drag. The estimated span efficiency was 80% for the full configurations. Sub-optimal efficiency was preferred to manufacturing complexity added by sweeping, twisting, or tapering the wings. The full drag polar for both planes are displayed in Figure 4.10 and were calculated by adding the induced drag from AVL and the parasitic drag from above. The drag polar indicated a maximum lift-to-drag ratio around 5.8 for the PA and 4.2 for the MSA. These relatively low values can be attributed to the large fuselage driven by Mission 2 and 3 payload volumes.

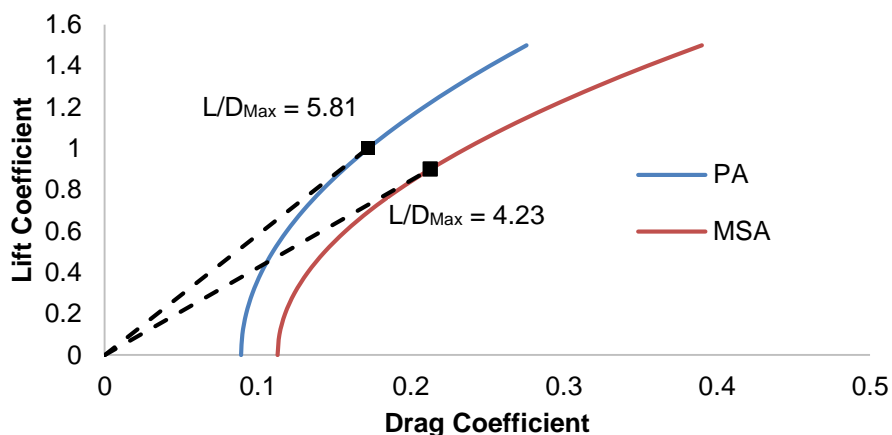


Figure 4.10: Full drag polar for both aircraft.

4.5 Stability and Control

Static and dynamic stability were analyzed to ensure that the aircraft would be able to successfully complete the flight missions. The fastest speeds, slowest speeds, heaviest weights, lightest weights, cruise, climbs, and turns were all considered, with results presented only for the critical flight condition.



4.5.1 Static Stability Analysis

Static stability was evaluated using the vortex lattice method implemented in AVL. The most demanding flight condition for trim was at the highest weight and lowest speed for both aircraft. Stability derivatives are given for these flight condition in Table 4.4. The aircraft are trimmed at this condition with a small elevator deflection and no extreme deflections were required for any of the cases analyzed. All cases indicate the aircraft are longitudinally, statically stable with a static margin of 18.2% for the PA and 12.7% for the MSA. All pitch, roll, and yaw derivatives are stable and within the acceptable range based on previous years' pilot feedback.

Table 4.4: Relevant stability coefficients and derivatives for static stability.

Parameter		Production Aircraft	Manufacturing Support Aircraft
Inputs	W_{total} (lbs.)	3.39	2.10
	V (ft/s)	45.6	25.5
Aerodynamic Parameters	C_L	0.97	1.04
	α (deg.)	11.0	15.0
	β (deg.)	0.0	0.0
Deflections	$\delta_{elevator}$ (deg)	-9.28	-8.27
	$\delta_{aileron}$ (deg)	0.0	0.0
Stability Derivatives	$C_{l,\beta}$ (rad $^{-1}$)	-0.14	-0.20
	$C_{L,\alpha}$ (rad $^{-1}$)	3.79	3.05
	$C_{m,\alpha}$ (rad $^{-1}$)	-0.69	-0.39
	$C_{n,\beta}$ (rad $^{-1}$)	0.15	0.18
Damping Derivatives	$C_{l,p}$ (rad $^{-1}$)	-0.35	-0.25
	$C_{m,q}$ (rad $^{-1}$)	-6.64	-5.47
	$C_{n,r}$ (rad $^{-1}$)	-0.19	-0.22
Static Margin	% Chord	18.2	12.7

4.5.2 Dynamic Stability Analysis

Knowing the trim conditions from the static stability analysis, the next step was to use the aerodynamic derivatives at the same trim conditions to investigate the dynamic behavior of the aircraft. The stability and control derivatives were obtained using AVL, the mass properties were obtained from the CAD file, and the stability characteristics were calculated using the six degrees of freedom linearized differential equation matrix found in Phillips' *Mechanics of Flight*, Section 9.8. The eigenvalues and eigenvectors of the matrix revealed that both aircraft are stable in the Short Period, Dutch Roll, and Roll modes, unstable in Spiral mode, and neutrally stable in Phugoid mode. The Spiral modes have a doubling time on the order of nine seconds, which is in line with past year's aircraft that flew without issue. The flight conditions used for this calculation were the same ones used in the static stability section, listed in Table 4.4. The dynamic stability characteristics are tabulated in Table 4.5.



Table 4.5: Dynamic stability analysis for least stable case.

		Longitudinal Modes		Lateral Modes		
Production Aircraft	Mode	Short Period	Phugoid	Dutch Roll	Roll	Spiral
	Damping Rate (s^{-1})	4.38	-0.02	0.31	1.81	-0.07
	Time to double/half (s)	0.15	38.30	1.02	0.38	9.57
	Damping Ratio (~)	0.70	-0.04	0.09	-	-
	Damped Natural Frequency (s^{-1})	4.47	0.43	3.29	-	-
	Undamped Natural Frequency (s^{-1})	6.26	0.43	3.3	-	-
Manufacturing Support Aircraft	Mode	Short Period	Phugoid	Dutch Roll	Roll	Spiral
	Damping Rate (s^{-1})	4.87	-0.02	0.57	4.07	-0.08
	Time to double/half (s)	0.14	30.14	1.23	0.17	9.21
	Damping Ratio (~)	0.93	-0.06	0.16	-	-
	Damped Natural Frequency (s^{-1})	1.96	0.39	3.54	-	-
	Undamped Natural Frequency (s^{-1})	5.25	0.39	3.58	-	-

4.6 Mission Performance

Mission 2 is flown with the MSA at MTOW. Mission 3 is flown with the PA at MTOW. Predicting aircraft performance in these missions is key. Lap trajectories for Missions 2 and 3 were estimated using the mission simulation described in Section 4.3, propulsion characteristics from MotoCalc, and aerodynamic characteristics of the airplane. Calculations for both aircraft were performed assuming an 11x8 propeller, a Cobra 2814/12 motor and a 7-cell 1500mAh NiMH battery. The estimated velocity profile for a single lap of Mission 2 is shown on the left of Figure 4.11 and that for a single lap of Mission 3 is shown on the right of Figure 4.11. Both figures include the takeoff run. “Valleys” in the velocity profiles correspond to the required turns over the course of each lap. The maximum velocity estimated for Mission 2 is 35.3 mph (51.8 ft/s), and the maximum velocity for Mission 3 is 43.1 mph (63.2 ft/s). The estimated lap times using optimal propellers for each mission’s first lap are shown in Figure 4.11. The analysis indicates that the PA can achieve the performance target of 3 laps in 5 minutes. The MSA can achieve 3 laps in 5 minutes at Mission 2 loading, indicating that it can easily meet the performance target of Mission 1 at a lighter loading. The estimated ground takeoff roll for Missions 2 and 3 are also included in Table 4.6. Both aircraft can achieve liftoff within the 100ft requirement.

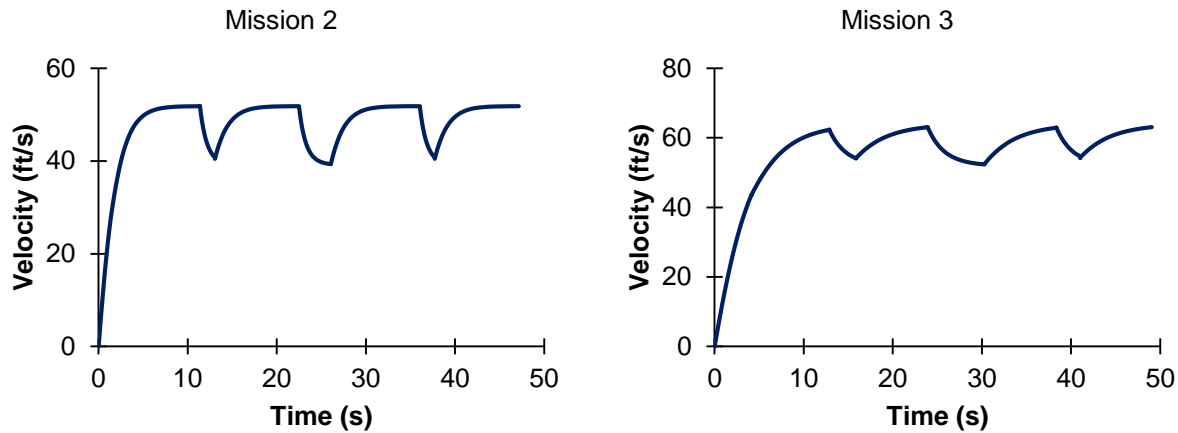


Figure 4.11: Simulation of Mission 2 and 3 lap trajectories.

Table 4.6: Predicted mission performance for each mission-propeller combination.

Mission	Propeller	TO Distance (ft)	Lap Time (s)
M2	11x7	20.7	47.2
M3	11x7	95.2	49.1

5. DETAIL DESIGN

5.1 Final Design

The aircraft dimensions did not vary between the preliminary and detailed design stages because the structural analysis and layout, component selection, and weight-balance calculations did not indicate major changes were needed. With the sizing completed, the final dimensional parameters are listed in Table 5.1. All wing and control surface chords were chosen to allow sufficient thickness for structure, embedded servos, and integration of the system, and then sized to provide stability at the constraint-derived wing area, leaving aspect ratio as a fallout variable. In summary, the final aircraft was designed for flight stability, simplicity, and structural efficiency.



Table 5.1: Final aircraft dimensional parameters.

Overall Dimensions (Production Aircraft)			Overall Dimensions (Manufacturing Support Aircraft)		
Length	33	in.	Length	41	in.
Wing L.E. X-Location	6	in.	Wing L.E. X-Location	9.5	in.
C. G. X-Location	8	in.	C. G. X-Location	12.5	in.
Static Margin	18.2%	chord	Static Margin	12.7%	chord

Wing (Production Aircraft)			Wing (Manufacturing Support Aircraft)		
Span	36	in.	Span	37.5	in.
Mean Chord	7.5	in.	Mean Chord	11.5	in.
Aspect Ratio	4.8	~	Aspect Ratio	3.26	~
Wing Area	270	in. ²	Wing Area	413	in. ²

Vertical Tail (Production Aircraft)			Vertical Tail (Manufacturing Support Aircraft)		
Span	6	in.	Span	7.5	in.
Chord	4	in.	Chord	7.5	in.
$\delta_{r, max}$	45	deg.	$\delta_{r, max}$	30	deg.
Reference Area	24	in. ²	Reference Area	56	in. ²

Horizontal Tail (Production Aircraft)			Horizontal Tail (Manufacturing Support Aircraft)		
Span	8	in.	Span	12	in.
Chord	4	in.	Chord	7.5	in.
$\delta_{e, max}$	45	deg.	$\delta_{e, max}$	30	deg.
Reference Area	32	in. ²	Reference Area	90	in. ²

5.2 Structural Characteristics

5.2.1 Layout and Design

The structural layout was created to ensure that all loads were accounted for and have an adequate load path to the major load-bearing components. The team divided all the loads the aircraft would see into three categories:

Motor Loads: Includes thrust, torque, and sustained vibrations. Components should be made of harder, quasi-isotropic materials such as plywood, and all fasteners must be locked.

Aerodynamic Loads: Includes wing and control-surface lift, drag, and moment, which translate to bending and torsion. Components can be anisotropic for added strength in the load direction.

Ground Loads: Includes aircraft weight and landing impact. Struts should be metal, which sustains impact by bending, not breaking.



The loads on each aircraft need to transfer into the major load bearing components, which includes the wing spar and fuselage attachment point. In flight, the wing may sustain up to a 2.5g load at maximum weight, based on the requirement of the wing tip test, therefore all loads from components not on the wing, such as payload and the empennage, traverse to the spar attachment point via the fuselage, as demonstrated in Figure 5.1. The fuselage is geometrically stiff due to the size required to accommodate the payload, making it an adequate load path. For the ground loads the fuselage has hard-points at the gear attachment locations to ensure impact loads do not damage any components.

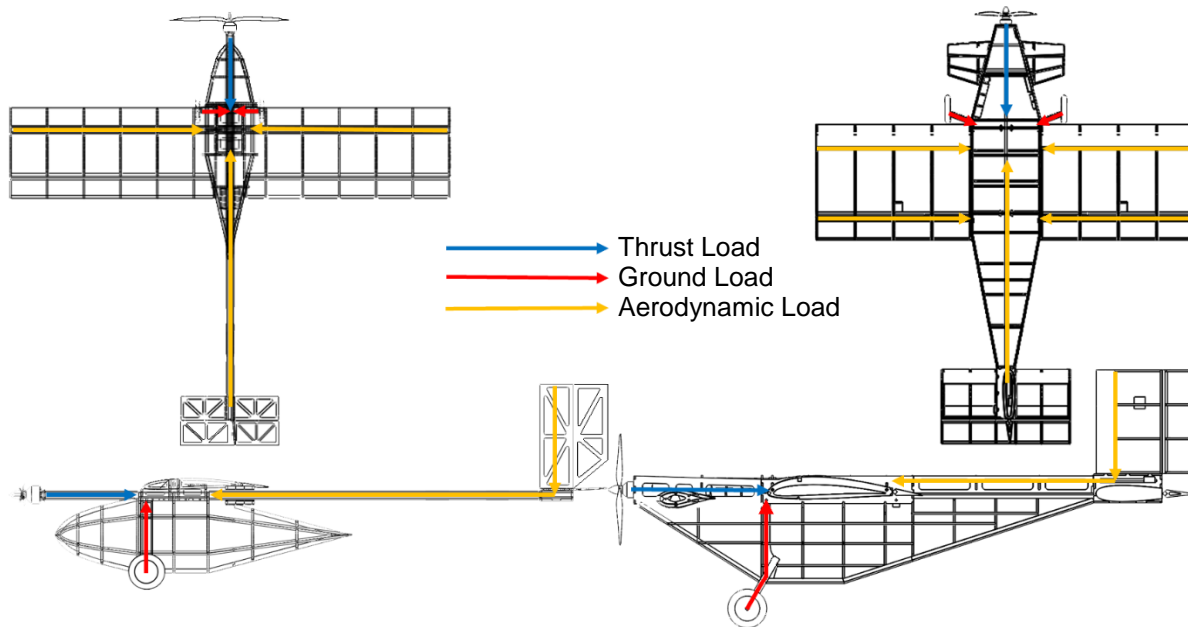


Figure 5.1: Load paths of major forces.

5.2.2 Operating Envelope

With the loads mapped and layouts complete, the structures of the aircraft were designed to withstand the design load of 2.5g at the maximum gross weight of 3.5 lbs for the PA and 2.5g at the maximum gross weight of 2.5 lbs for the MSA. This translates to a 66-degree bank angle for sustained level turns. It was not necessary to analyze the MSA in its unloaded state because the performance is similar while the weight is lower. The ultimate load could not be well quantified because balsawood has significant variation in ultimate strength. The 2.5g design load-limit at small deflections was retained as the maximum positive load envelope. The negative load limit was defined at -1g for both aircraft to prevent the wing attachment area from failing in compressive buckling. The defining structural limits were combined with aerodynamic performance limits at each mission to construct the V-n diagram displayed in Figure 5.2.

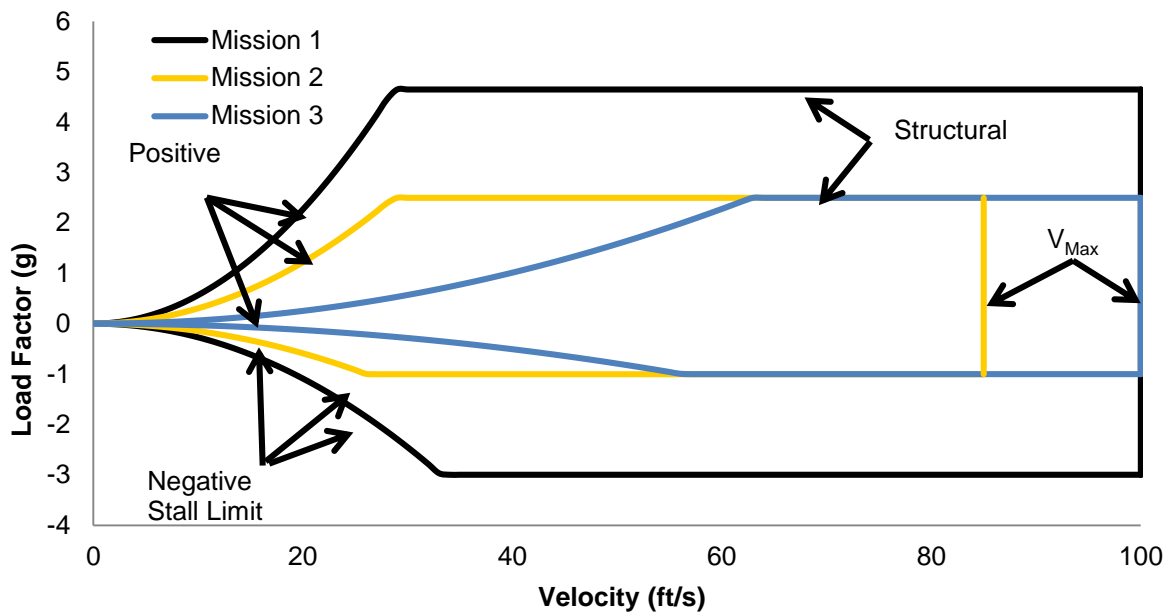


Figure 5.2: V-n Diagram showing loading as a function of velocity for Missions 1, 2, and 3.

5.3 System and Subsystem Design/Component/Selection/Integration

To finalize the aircraft design, the following subsystems were analyzed with greater detail: radio controller, servos, main wing, propulsion system, landing gear, and the structural architecture/assembly for each of these components. Fuselage, wing, motor mount, empennage, payload enclosure, receiver and transmitter, propulsion, and servos.

5.3.1 Fuselage

The PA is a stick and wing design. The fuselage uses balsa for the structural members and a carbon fiber rod as the primary structure. The center body is designed to interface the wing, servo, primary structure, landing gear and payload bay while minimizing weight. The CAD model is developed such that the center body has interlocking slots, allowing parts to fit together like a jigsaw puzzle. This method allows for the grain direction of the balsa to be appropriate for load transfer and more efficient manufacturing. The MSA is a hybrid design. A bulkhead-stringer design is used for the payload compartment, allowing for both minimum weight and adequate load transfer, while the main load-bearing structure follows a stick and wing paradigm. The interlocking method used for the PA is reproduced for the MSA. The CAD models of the Fuselages of the PA and MSA can be found in Figure 5.3.

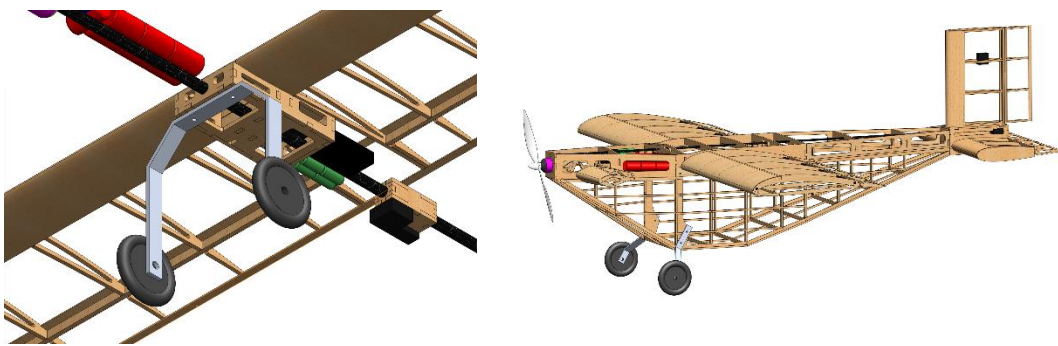


Figure 5.3: PA and MSA fuselage CAD.

5.3.2 Wing

The PA wings follow a conventional rib and spar layout. The main structure is a set of two balsa spars located at the quarter chord reinforced with flat carbon fiber rectangular rods. An aft spar is located at the three-quarter chord for the aileron attachment. Balsa was selected as the material for the spars and ribs due to its unique combination of strength, weight, and machinability. The MSA wings follow a similar design are designed to slide over the PA wings and transfer load through concentric carbon fiber tubes placed at the leading and trailing edge. Both are shown in Figure 5.4 below.

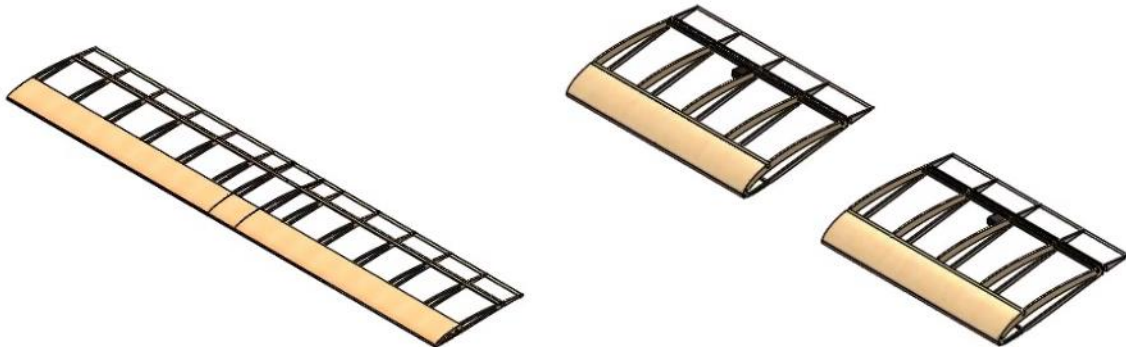


Figure 5.4: Wing design and structural layout.

5.3.3 Motor Mount

The PA motor mount is connected directly to the end of the carbon fiber rod. Four pieces of 1/8th inch thick plywood are glued together as a composite firewall capable of withstanding motor thrust and torque loads. Four bolt holes were cut into the firewall to mount the motor. The MSA motor mount motor attaches directly to 1/8th inch thick plywood plate. This plate is connected directly to the carbon-fiber rod of the main structure with epoxy. This is shown in Figure 5.5 below.

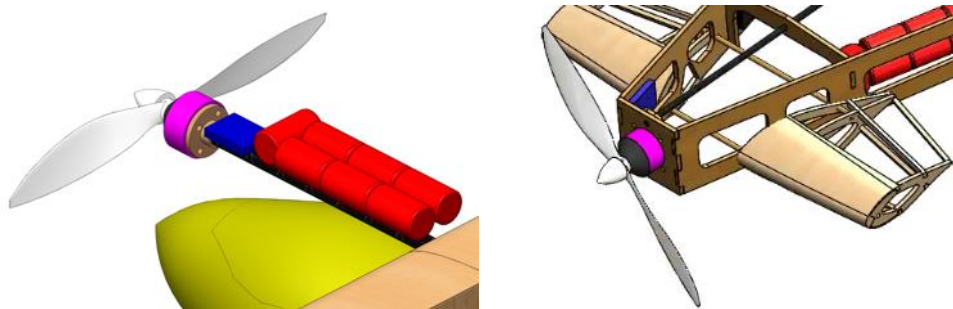


Figure 5.5: Motor mount assembly.

5.3.4 Empennage

The PA empennage was designed in CAD to minimize size. Flat balsa sheets with lightening holes were used as flat-plate airfoils, with decreased control surface effectiveness mitigated by increasing available deflection. The MSA empennage was designed in CAD to envelope the PA empennage while being lightweight. The construction uses similar materials and construction techniques as the wings, with balsa wood used for the majority of the structure, augmented by plywood members in key locations. The bottom of the empennage hinges to fit the PA empennage. This design is shown in Figure 5.6 below.

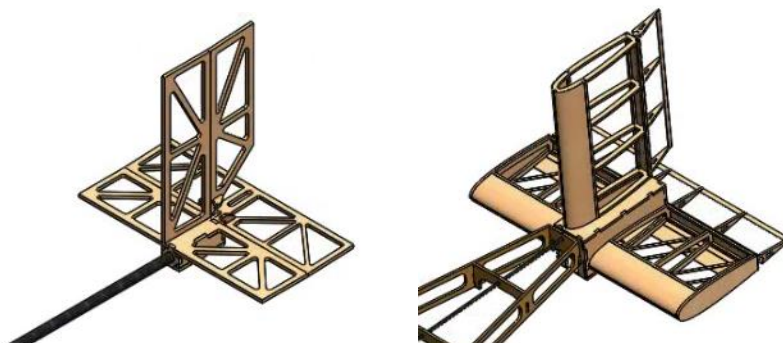


Figure 5.6: Empennage assembly.

5.3.5 Payload Enclosure

The PA payload enclosure was designed to have low drag and low weight without compromising robustness. An aerodynamic shape was made in CAD, then machined out of foam and coated with epoxy to create a mold for thermoformed plastic manufacturing. The enclosure opens along one side to allow access for securing the Mission 3 payload. This is shown in Figure 5.7 below.

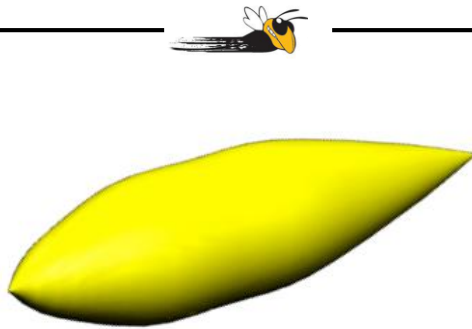


Figure 5.7: Payload Enclosure of the Production Aircraft.

5.3.6 Receiver and Transmitter Selection

The receiver selected is the Futaba R6008HS, as it provides the required failsafe mechanism with minimum weight. *Buzzdryoshka* used a Futaba T8FG 2.4 GHz radio transmitter to communicate with the receiver.

5.3.7 Propulsion System

A 7-Cell Elite 1500 mAH NiMH battery pack was selected to minimize weight while maintaining enough voltage to achieve mission requirements. A variety of motors and propellers were analyzed using the MotoCalc program, as described in Section 4.2.2. Two were selected for further testing, as described in Section 7.2. The Cobra 2814/12 motor was chosen for its weight, size and static thrust. The APC 11x8 propeller was chosen for its desired ratio between thrust required for cruise speed and thrust required for takeoff. The final selected propulsion system consists of a Cobra 2814/12 motor, 7 cell Elite 1500 mAH NiMH battery pack, a Phoenix Edge Lite 50 speed controller with the APC 11x8 propeller.

5.3.8 Servo Selection and Integration

The Futaba S3114 was selected as the servo for the aileron and elevator. These servos were selected by analyzing hinge-moments for each control surface using AVL and then finding servos that had sufficient control power to handle the calculated moments, with the lightest weight possible. The selected components are tabulated in Table 5.2:

Table 5.2: Selected components.

Components	Description
Motor	Cobra 2814/12
Battery	7 cell ELITE 1500
Speed Controller	Phoenix Edge Lite 50
Receiver	Futaba R6008HS
Transmitter	Futaba T8FG
Aileron Servo	Futaba S3114
Elevator and Rudder Servos	Futaba S3114



5.4 Weight and Balance

An important aspect of stability is correct center of gravity (C.G.) location. To estimate the C.G., a simple calculator was created that consisted of a list of all components, their weights, and their locations along the x-axis and z-axis. Component weights were first estimated using the CAD model and then confirmed with the physical vehicle. Table 5.3 contains the results for all mission scenarios for the PA. Table 5.4 contains those for the MSA. The x-axis was measured positive aft of the nose of the aircraft and the z-axis was measured positive above the chord-line of the wing. The predicted C.G. locations from the CAD of the PA and MSA are shown in Figure 5.8.

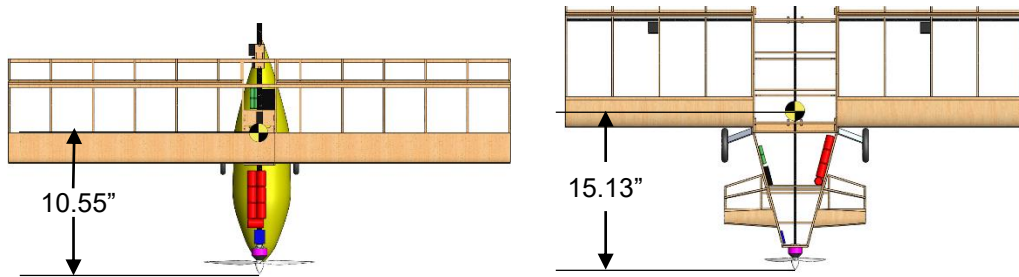


Figure 5.8: PA and MSA C.G. location from CAD model.

Table 5.3: Weight and balance chart – Production Aircraft.

Empty Weight					
Component	Weight (lbs)	C.G. loc.(in, x-axis)	Moment (in-lbs, y-axis)	C.G. loc. (in, z-axis)	Moment (in-lbs, x-axis)
Fuselage	0.02	12.00	0.24	0.00	0.00
Empennage	0.09	32.00	2.88	0.00	0.00
Speed Controllers	0.04	6.00	0.24	0.00	0.00
Receiver	0.03	11.00	0.33	0.00	0.00
Propeller	0.04	0.25	0.01	0.00	0.00
Wing	0.12	10.75	1.24	0.00	0.00
Carbon Fiber Rod	0.06	17.00	0.94	0.00	0.00
Aileron Servo 1	0.02	12.50	0.21	0.13	0.00
Aileron Servo 2	0.00	0.00	0.00	0.00	0.00
Tail Servo 1	0.02	16.00	0.27	0.13	0.00
Tail Servo 2	0.02	16.00	0.27	0.00	0.00
Main Gear	0.13	8.50	1.06	-4.00	-0.50
Tail Gear	0.01	32.50	0.16	-0.13	0.00
Motor	0.15	1.75	0.25	0.00	0.00
Receiver Battery	0.10	5.00	0.50	0.00	0.00
Aircraft Totals	0.82	10.55	8.61	-3.88	-0.50
Mission 3					
Battery	0.37	6.25	2.33	0.38	0.14
Payload	2.20	11.40	25.08	-2.75	-6.05
Aircraft Totals	3.39	10.63	36.02	-1.89	-6.41



Table 5.4 shows that the battery must move significantly in order to balance C.G. for each mission. This is necessary due to the insertion of the PA during Mission 2, where the C.G. is lowered by 1.07. This was not found to be a problem during flight testing, and the team considers the aircraft safe.

Table 5.4: Weight and balance chart – Manufacturing Support Aircraft.

Empty Weight					
Component	Weight (lbs)	C.G. loc.(in, x-axis)	Moment (in-lbs, y-axis)	C.G. loc. (in, z-axis)	Moment (in-lbs, x-axis)
Fuselage	0.17	19.00	3.23	-3.00	-0.51
Empennage	0.04	39.00	1.56	2.50	0.10
Speed Controllers	0.04	10.00	0.40	0.00	0.00
Receiver	0.03	10.00	0.30	0.00	0.00
Propeller	0.04	0.50	0.02	0.00	0.00
Wing	0.20	18.00	3.60	0.00	0.00
Carbon Fiber Rod	0.06	21.50	1.36	0.75	0.05
Aileron Servo 1	0.02	20.00	0.34	0.00	0.00
Aileron Servo 2	0.02	20.00	0.34	0.00	0.00
Tail Servo 1	0.02	39.25	0.67	0.13	0.00
Tail Servo 2	0.02	39.50	0.67	6.00	0.10
Main Gear	0.11	10.50	1.18	-7.50	-0.84
Tail Gear	0.01	42.00	0.21	-1.50	-0.01
Motor	0.15	1.75	0.25	0.00	0.00
Receiver Battery	0.10	12.00	1.20	0.00	0.00
Aircraft Totals	1.01	15.13	15.33	-2.63	-1.11
Mission 1					
Battery	0.37	10.00	3.73	0.25	0.09
Payload	0.00	0.00	0.00	0.00	0.00
Aircraft Totals	1.39	13.75	19.06	-0.73	-1.02
Mission 2					
Battery	0.37	7.15	2.67	0.25	0.09
Payload	0.72	15.25	10.92	-3.88	-2.77
Aircraft Totals	2.10	13.75	28.92	-1.80	-3.79

5.5 Flight and Mission Performance

5.5.1 Flight Performance

The flight performance of the aircraft may be described by the point performance of the vehicle. Key aspects include the velocity envelope and turn performance, as well as takeoff distance and stall speed. These are given below in Table 5.5.



Table 5.5: System flight performance parameters for each mission.

	Mission 1	Mission 2	Mission 3
Weight (lbs)	1.39	2.10	3.53
W/S (psf)	0.47	0.71	1.81
TOFL (ft)	6.72	20.70	95.20
V_{stall} (ft/sec)	19.30	23.15	41.50
V_{max} (ft/sec)	52.50	51.80	61.00
Load Factor	4.50	2.50	2.50
Turn Radius (ft)	17.10	33.88	50.43
Time for 360 (s)	2.15	4.26	5.19

Weight represents the Mission 1, 2, and 3 gross take-off weights. Both wing loading and stall speed are calculated at 1g assuming steady level flight while using an estimation of C_{Lmax} created with AVL modeling and section lift data. Takeoff field length (TOFL) was computed via numerical integration in MATLAB using the drag polar, friction coefficients, and thrust available from the wind tunnel test data. Load factor for each mission is the maximum allowable based on results from the V-n Diagram. In all cases, the load factor is intended to represent a maximum. Flight-test data indicates that in-flight loads will be lower. The turn radius and time to complete a 360 degree turn were calculated for each mission using the mission's expected maximum velocity and allowable load factor. The maximum velocity of the aircraft occurs at the point when the thrust required is equal to the thrust available. Thrust required is calculated using Equation 5.1 where $C_{D,0}$ and e are calculated in Section 4.4.3.

$$T_R = \frac{1}{2} \rho V^2 S C_{D,0} + \frac{2W}{\rho V^2 S \pi A Re} \quad (5.1)$$

Thrust available as a function of velocity was computed using MotoCalc for both propellers considered and plotted in Figure 5.9, along with the thrust required curves in steady-level flight for the PA and MSA.

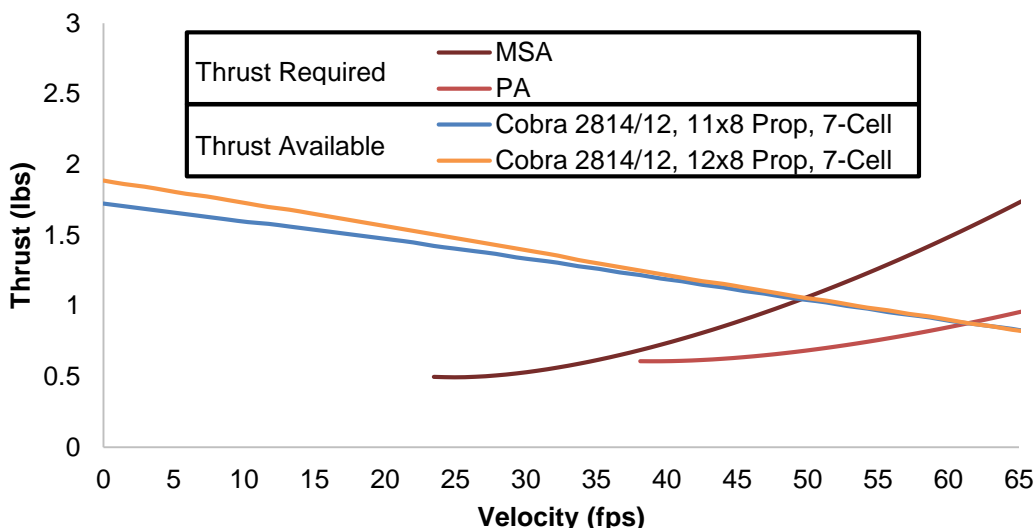


Figure 5.9: Thrust available and thrust required versus velocity.



Figure 5.9 shows that for a constant motor, the 11x8 and 12x8 propellers achieve similar performance at velocity greater than 35 fps. Since the PA stalls at ~38 fps and the propulsion system of the MSA is overpowered, the team preferred the smaller propeller for ease of packaging.

5.5.2 Mission Performance

The mission model described in Section 4.3 was used to estimate the final mission performance of the aircraft. The computed lap times represent an estimate that combines aerodynamics from AVL, power and current characteristics from MotoCalc, and the physics of the mission model as described in Section 4.3. Figure 5.10 displays the projected first lap trajectories for Missions 1, 2 and 3, with an initial ramp-up following takeoff and dips in velocity occurring at the turns. The remaining laps for Missions 1 and 3 are faster because they do not include takeoff. Table 5.6 shows the resulting estimated performance for each of the three missions with the selected propellers. The table also includes scoring estimates based on the updated analysis.

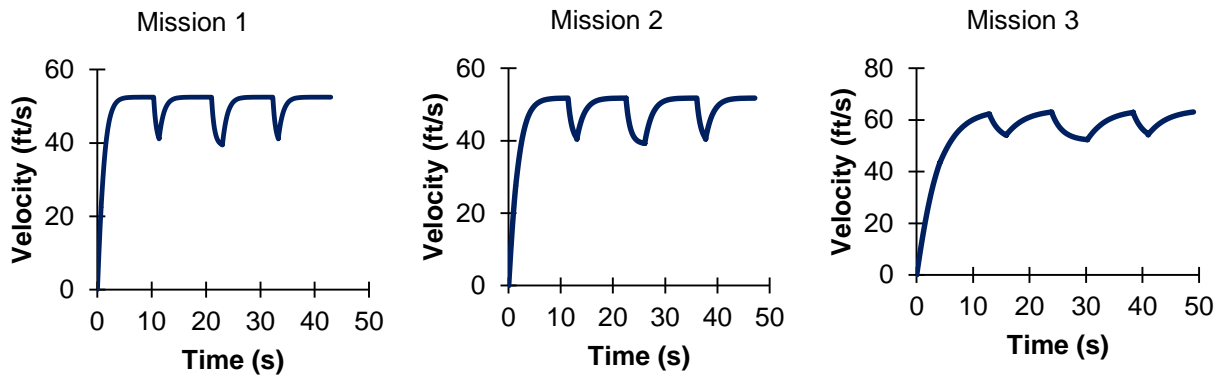


Figure 5.10: Simulation of Mission 1, 2 and 3 lap trajectories.

Table 5.6: Aircraft mission performance parameters.

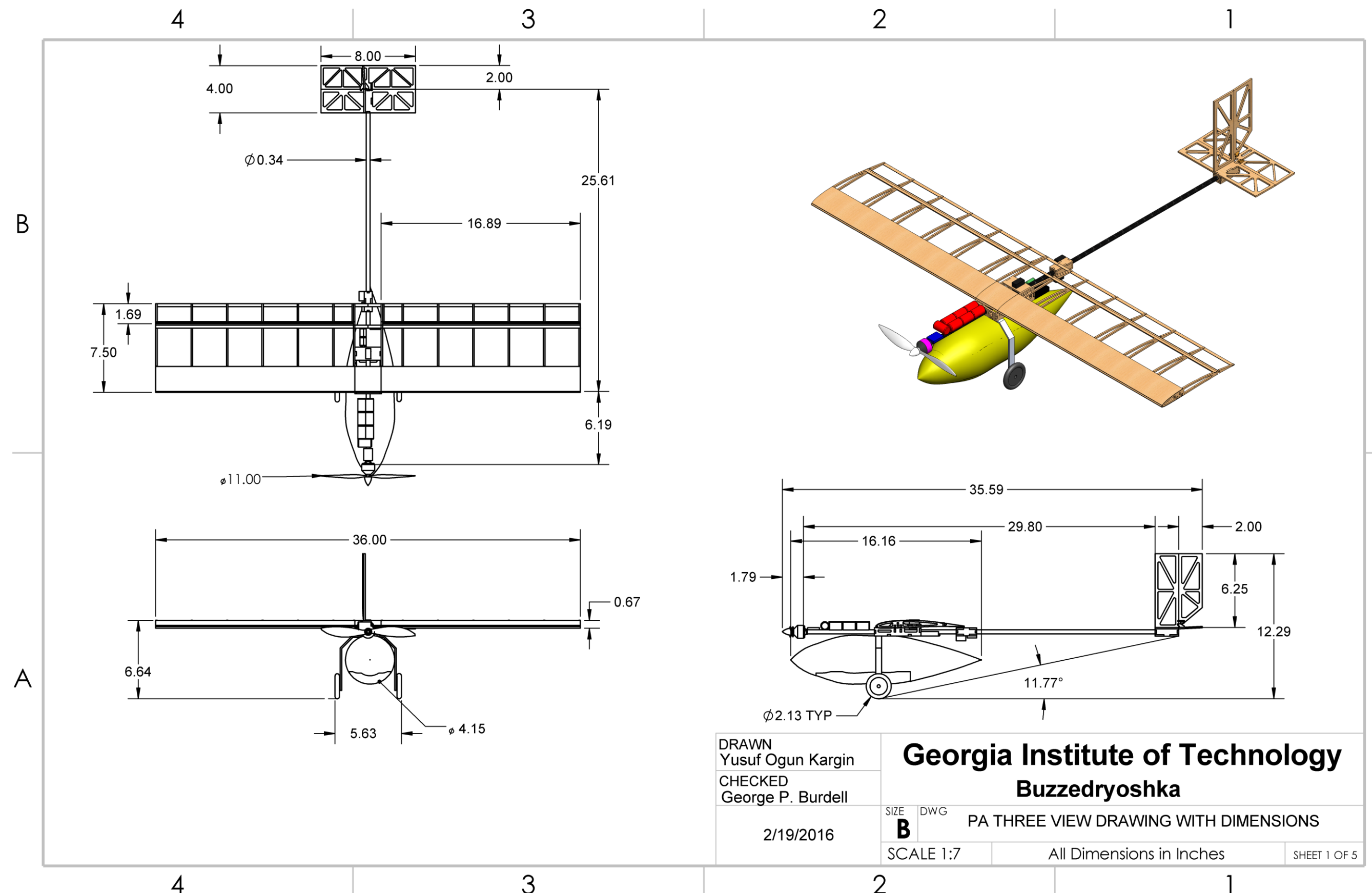
Mission Parameter	Mission 1	Mission 2	Mission 3
W/S (psf)	0.469	0.709	1.81
Propeller Selection	11x8	11x8	11x8
Max Current (Amp)	19	19	19
Static Thrust (lbs)	1.89	1.89	1.89
1 st Lap Time (sec)	43.0	47.2	49.1
Mission Performance	3 laps in 5 minutes	1 lap	3 laps in 5 minutes
Mission Score	2.0	4.0	2.0
RAC	0.961	0.961	0.961



Based on the updated mission performance estimates shown in Table 5.6, the estimated total mission score is 10. After normalization by RAC the score stands at 10.4.

5.6 Drawing Package

The following five pages illustrate the detailed CAD of *Buzzedryoshka* system. The first and second sheets have the three-view diagram with relevant dimensions of the PA and the MSA respectively. The third and fourth sheets show the structural arrangement of all major components and the systems layout and location for the PA and the MSA respectively. The fifth sheet displays the payload arrangements for both aircraft.



4

3

2

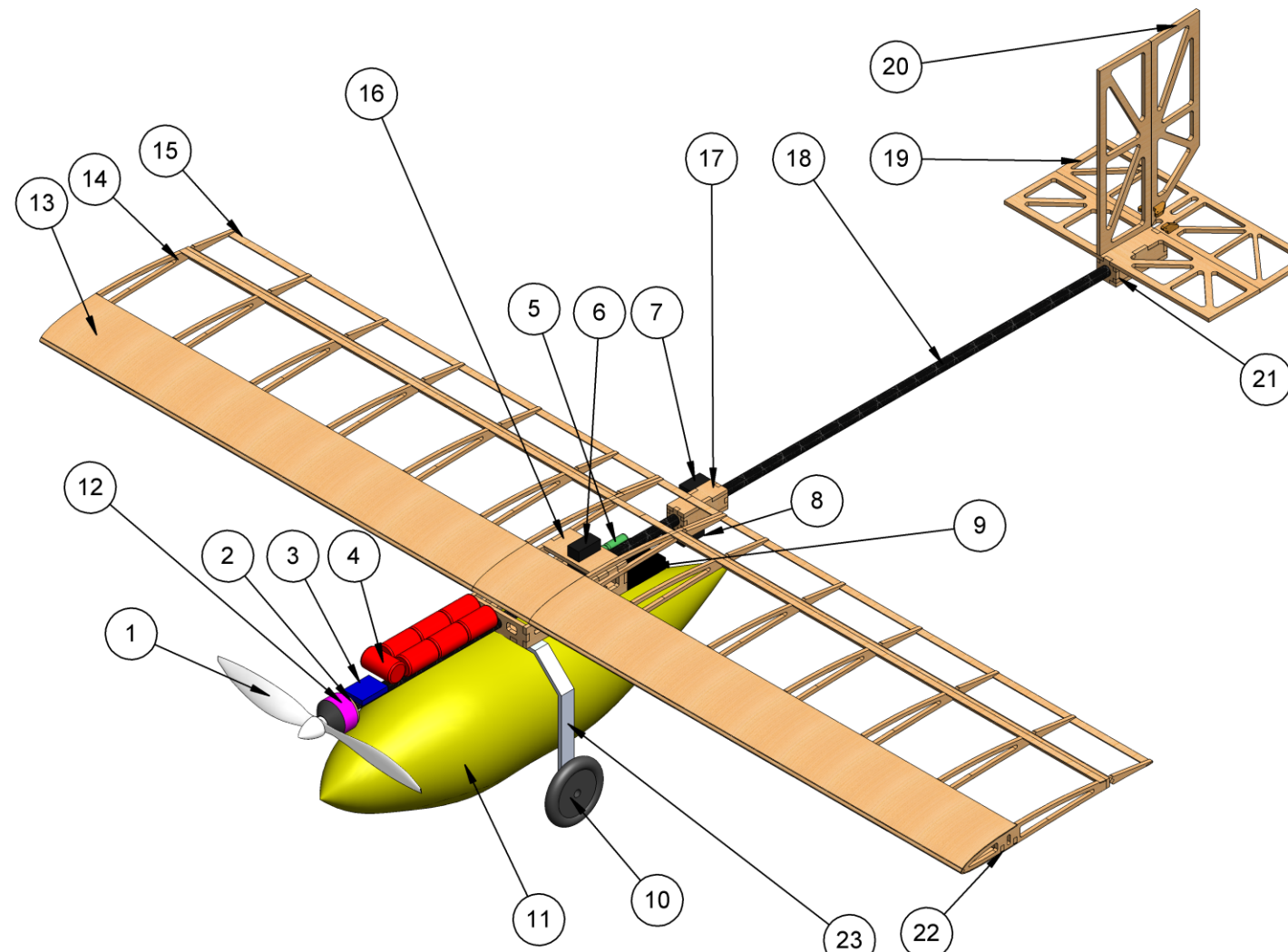
1

B

A

SYSTEMS LIST

Item	Qty.	Item Name	Description
1	1	Propeller	APC 11x8
2	1	Motor	Cobra 2814
3	1	Speed Controller	Phoenix 35A
4	1	Main Battery Pack	7 cell 1500 mAh
5	1	Receiver Battery Pack	4 cell 400 mAh
6	1	Aileron Servo	Futaba S3114
7	1	Rudder Servo	Futaba S3114
8	1	Elevator Servo	Futaba S3114
9	1	Receiver	Futaba H6008S
10	2	Wheel	Rubber Tires
11	1	Payload Fairing	Plastic



PARTS LIST

Item	Qty.	Item Name	Description
12	1	Motor Mount	Plywood
13	1	Wing Sheeting	Balsa
14	14	Wing Rib	Balsa
15	2	Aileron	Balsa
16	1	Fuselage Box	Balsa
17	1	Servo Box	Balsa
18	1	Boom	Carbon Fiber
19	1	Elevator	Balsa
20	1	Rudder	Balsa
21	1	Empennage	Balsa
22	2	Spar Capping	Carbon Fiber
23	1	Main Landing Gear Strut	Aluminum

DRAWN
Yusuf Ogun Kargin

CHECKED
George P. Burdell

2/19/2016

Georgia Institute of Technology
Buzzedryosha

B DWG
PA Structural Arrangement and Systems Layout Drawing

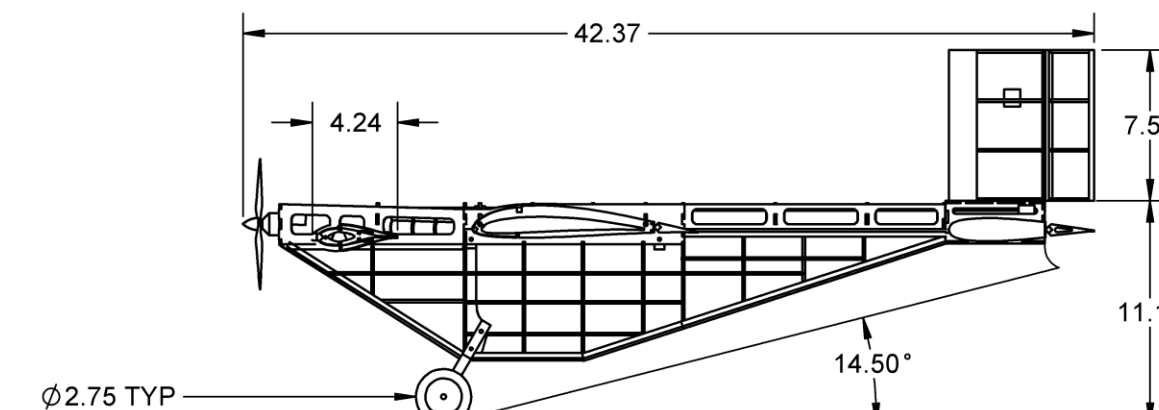
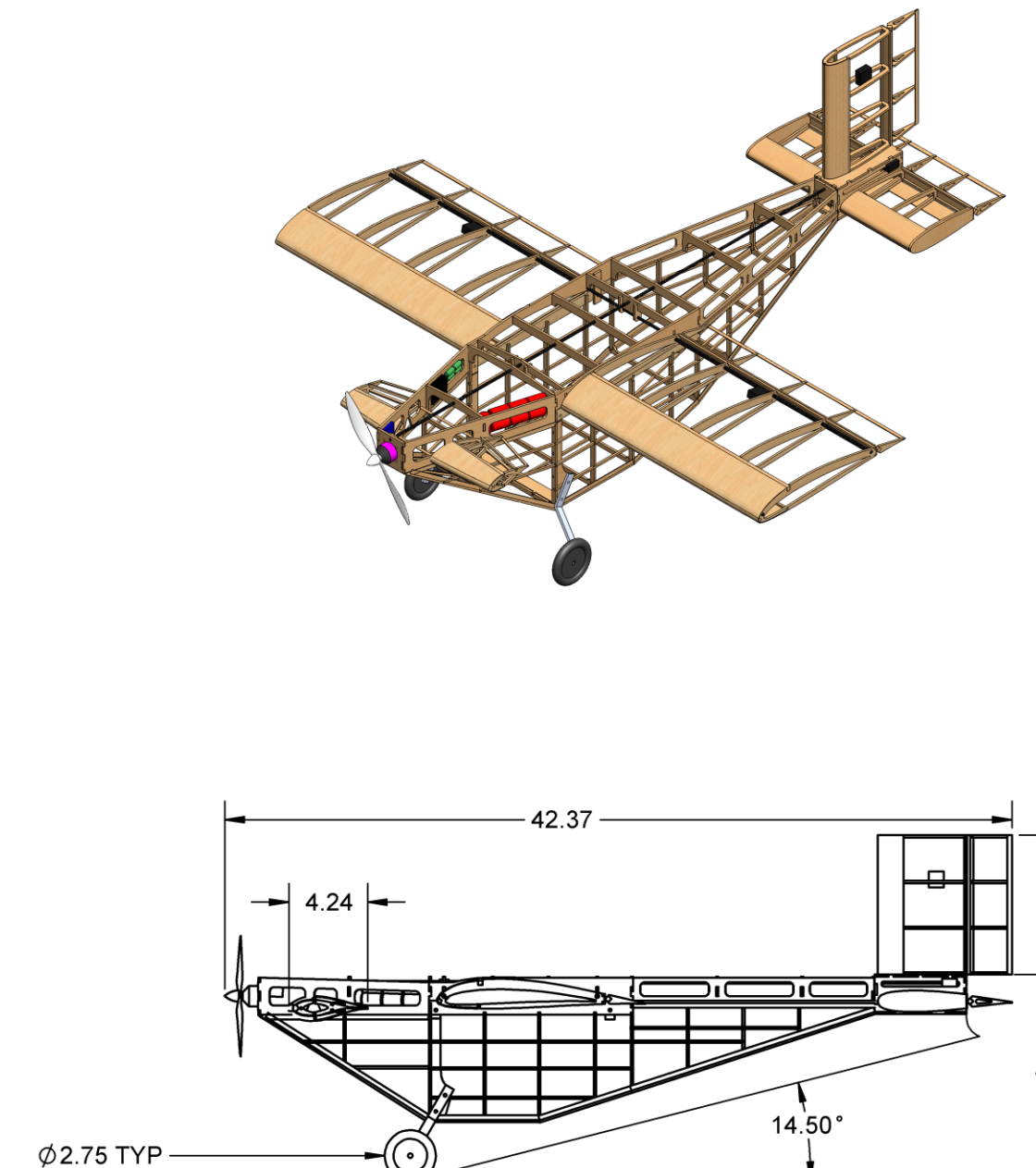
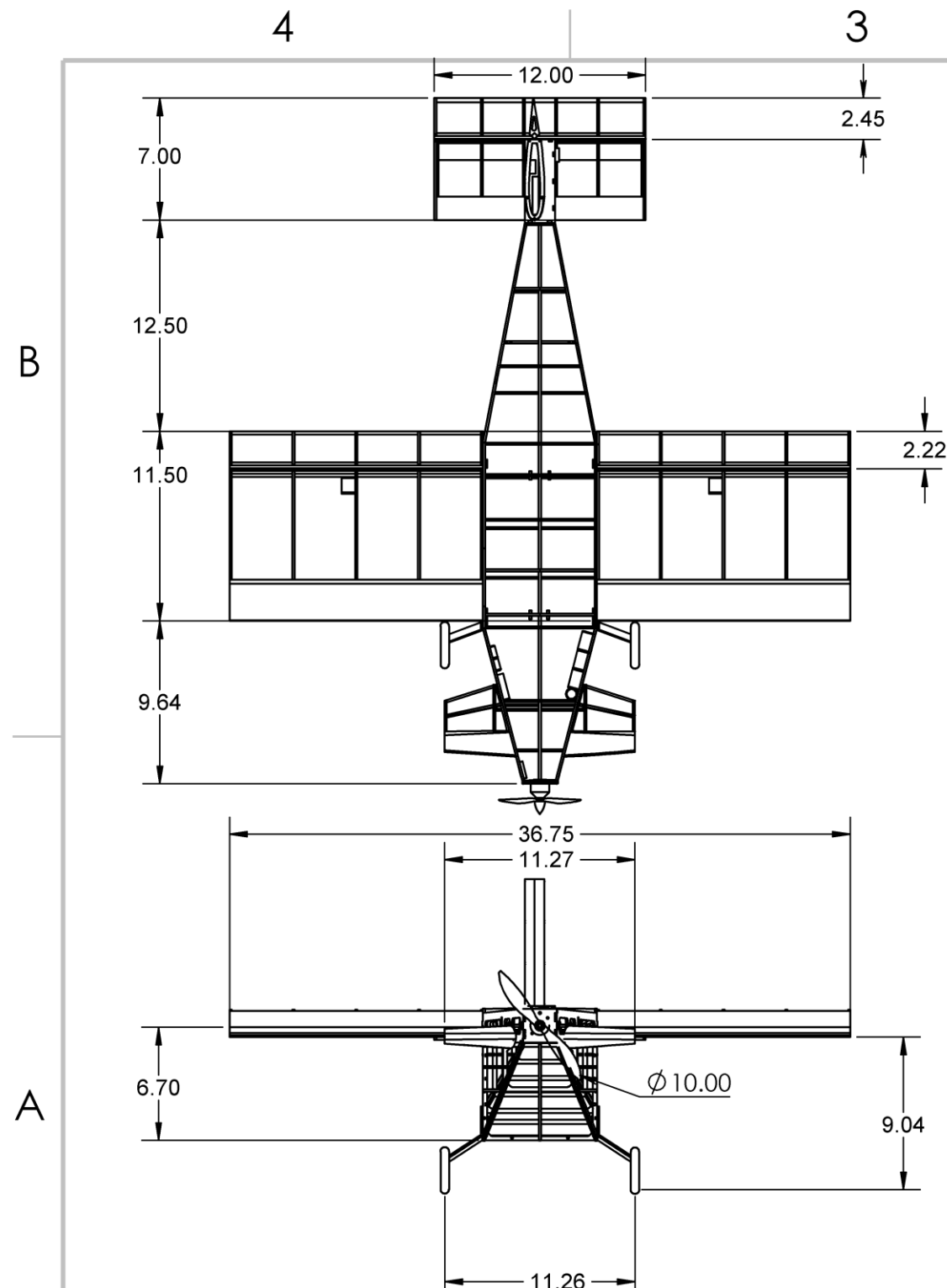
SCALE 1:3 All Dimensions in Inches SHEET 2 OF 5

4

3

2

1



Georgia Institute of Technology
Buzzedryoshka

DRAWN Osvaldo Armas	SIZE DWG
CHECKED George P. Burdell	B
2/19/2016	MSA Three View Drawing with Dimensions
SCALE 1:8	All Dimensions in Inches
SHEET 3 OF 5	

4

3

2

1

B

B

SYSTEMS LIST			
Item	Qty.	Part Name	Description
1	1	Propeller	APC 11x8
2	1	Motor	Cobra 2814
3	1	Speed Controller	Phoenix Edge Lite 50
4	1	Receiver	Futaba R6008HS
5	1	Receiver Battery Pack	4 cell 400 mAh
6	1	Aileron Servo	Futaba S3114
7	1	Rudder Servo	Futaba S3114
8	1	Tail Bottom Lid	Balsa
9	1	Elevator Servo	Futaba S3114
10	1	Detachable Top Fuselage	Balsa
11	2	Detachable Wing	Balsa
12	1	Main Battery Pack	7 cell 1500 mAh
13	2	Wheel	Rubber Tire
14	1	Bottom Fuselage	Balsa
15	2	Detachable Canard	Balsa

A

A

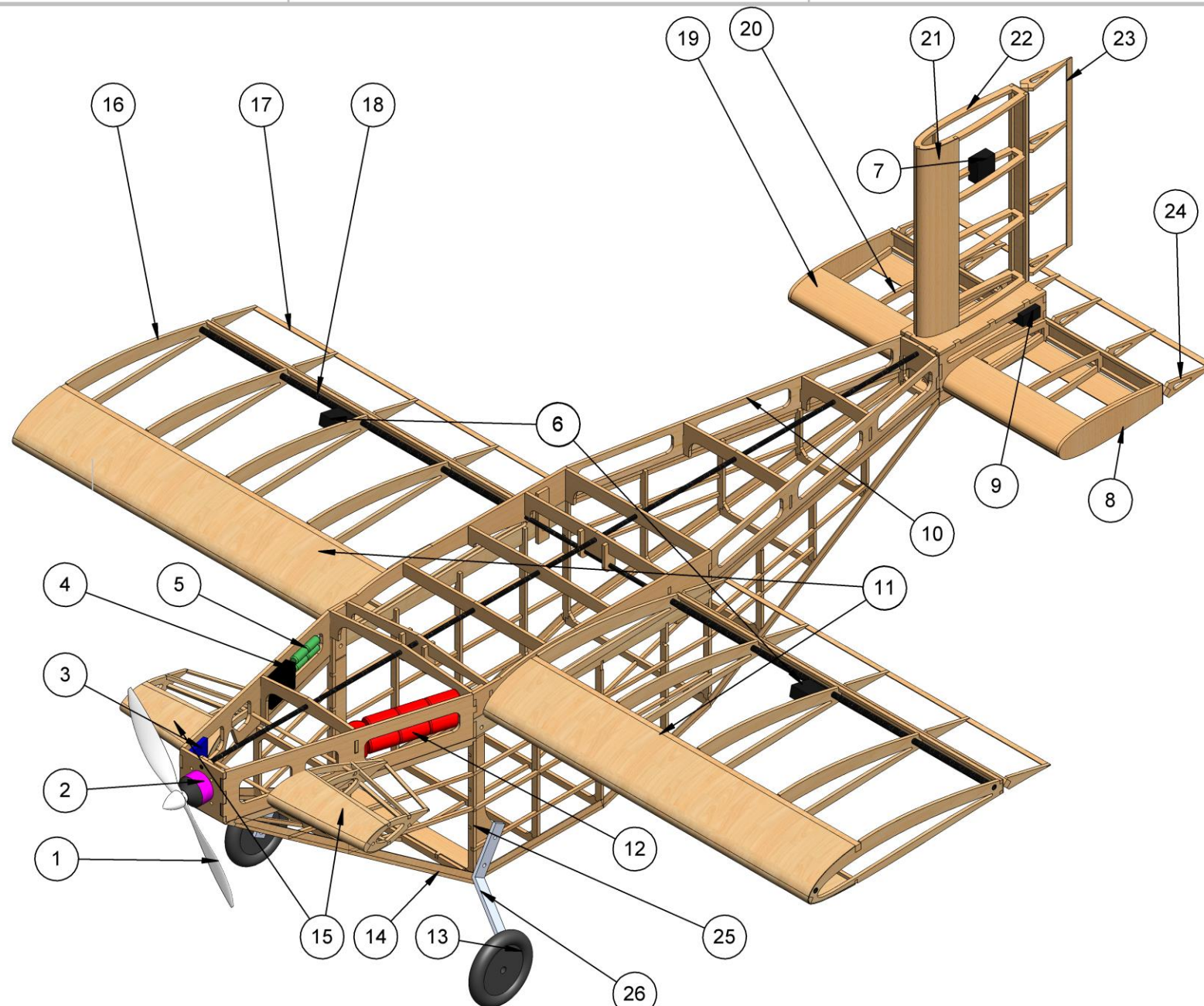
PARTS LIST			
Item	Qty.	Part Name	Description
16	10	Wing Rib	Balsa
17	2	Aileron	Balsa
18	4	Wing/Fuselage Joint	Carbon fiber Rod
19	2	Horizontal Tail Sheeting	Balsa
20	6	Horizontal Tail Rib	Balsa
21	1	Vertical Tail Sheeting	Balsa
22	4	Vertical Tail Rib	Balsa
23	1	Rudder	Balsa
24	1	Elevator	Balsa
25	1	Bulkhead	Plywood
26	2	Landing Gear Strut	Aluminium

4

3

2

1

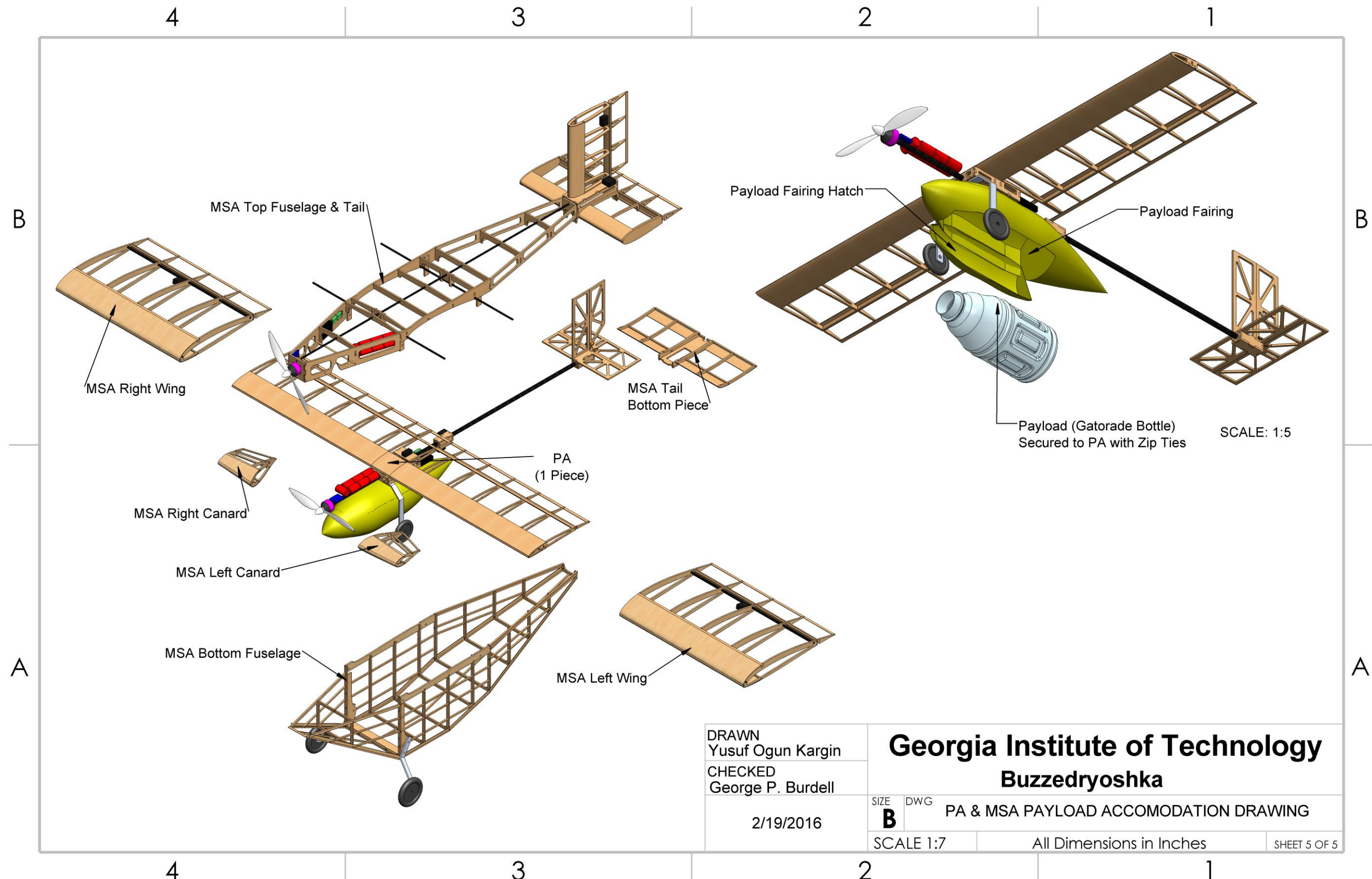
DRAWN
Yusuf Ogun KarginCHECKED
George P. Burdell

2/19/2016

Georgia Institute of Technology
Buzzedryoshka

SIZE DWG
B MSA Structural Arrangement and Systems Layout Drawing

SCALE 1:4 All Dimensions in Inches SHEET 4 OF 5





6. MANUFACTURING PLAN AND PROCESSES

In order to design and build a competitive aircraft, the team considered various manufacturing processes and materials. The manufacturing process selected represented the best combination of weight, reparability, ease of manufacturing, team experience with the process, and cost.

6.1 Manufacturing Processes Investigated

The team had a wealth of experience using the built-up balsa wood manufacturing technique. However, there were other viable manufacturing processes that could be superior. These processes were considered and qualitatively compared to the built up balsa technique using Figures of Merit, detailed below and summarized in Table 6.1.

Weight: similarly to conceptual design, weight is still the most important factor for any design decision, and is assigned a FOM of 5.

Reparability: With ever-present unknown factors, the reparability of the aircraft in case of an accident or a crash has to be accounted for, and was assigned a FOM of 2.

Ease of Manufacture: The ability to produce the aircraft to specification is critical to meet expected performance, and is directly related to Ease of Manufacture. It was therefore assigned a FOM of 3.

Experience: The team's knowledge was given some weighting because it relates to the ability of team members to produce quality results, as well as to refine existing techniques. However, since the team is always willing to learn new techniques, experience was only assigned a FOM of 2.

Cost: Keeping in mind that the team had limited resources, cost was inevitably added as a FOM. However, since the team emphasizes winning above all, cost was assigned a FOM of 1.

Table 6.1: Manufacturing FOM weighting.

Figure of Merit	0	1	2	3	4	5
Weight						5
Ease of Manufacture				3		
Reparability			2			
Experience			2			
Cost		1				

These Figures of Merit were used to investigate the manufacturing processes and materials common to remote control aircraft construction that were investigated detailed below.

Built-up Balsa: Stocks of competition grade balsa wood are laser cut from CAD models and glued together using cyanoacrylate (CA) adhesive to form the skeleton of the aircraft. It is then locally reinforced with more balsa or carbon fiber if necessary, and coated with Ultracote heat shrink film.



Foam Core Composite: Large blocks of foam are cut with a hot-wire or Computer Numerically Controlled (CNC) router to form the basic shape of the aircraft. Structural reinforcements are locally added if needed, and the entire foam-core is coated in fiberglass or carbon fiber, adding strength while providing an aerodynamic skin.

Molded Composite: This process is similar in principle to a foam core; however, the foam parts are only used to mold the composites and are then removed, with the fiberglass or carbon fiber acting as the primary structure.

Thermoformed Plastic: The process starts with a thin sheet of plastic is heated until it becomes moldable. The plastic then made to conform around the mold by application of a strong vacuum and is allowed to cool and assume a new shape. This process is ideal for making fairings and other non-structural components.

The processes were evaluated against each other by assigning each one a FOM score, with a score of five indicating a superior choice, three an average choice, and one equaling an inferior choice. All methods were assumed to result in an aircraft designed for an identical load. The results of the comparison are summarized in Table 6.2.

Table 6.2: Weighting for various manufacturing techniques.

FOM	Value	Manufacturing Process			
		Built-up Balsa	Foam Core Composites	Molded Composites	Thermoformed Plastic
Weight	5	5	3	5	5
Ease of Manufacture	3	3	3	1	2
Reparability	2	3	1	1	5
Experience	2	5	3	3	1
Cost	1	5	3	1	5
Total	13	55	35	37	48

Based on the Figures of Merit, built-up balsa was considered the best method for the plane manufacturing. To further confirm this choice, the team laid-up a molded composite wing section, the second-best candidate of the assessment above. The section consisted of 3 oz/yd² fiberglass with 1/32" balsa core, and resulted in an area density of 0.12 lbs per square foot of skin. With nearly 10 ft² of wetted area, the wing alone would weigh 1.2 lbs, more than the entire balsawood structure of the aircraft as-built. Therefore, the built-up balsa technique was used to construct the aircraft.

6.2 Manufacturing Processes Selected

The team used the above comparison to optimize the built-up balsa technique to achieve the most competitive aircraft by having the lightest structure possible in accordance with competition rules without sacrificing structural integrity. This optimized technique is detailed in Table 6.3 below:



Table 6.3: Built-up balsa manufacturing technique.

Manufacturing Component	Material / Technique
Principal material	Competition Grade balsa wood
Other materials	Local fiber reinforcements
Adhesive	CA, or epoxy if needed
Coating	Ultracote
Part manufacture	CAD-guided laser cutting
Part assembly	Designed-to-fit jigsaw pieces

Of the many different ways to apply built-up balsa, the team chose specific techniques and materials that would minimize the aircraft structure's weight without compromising its strength. These strategies are:

Selective Material Use: Since balsa wood can vary significantly in density and strength, the team sorted its entire stock of balsa by weight. The lightest pieces were selected for construction and were cut using the team's laser cutter, with the lightest of the cut parts reserved for the final competition aircraft.

Local Reinforcements: Due to the very low density of balsa used, the aircraft structure lacked strength in several key locations. Rather than compensate by over-building the entire aircraft, these locations were reinforced with composite or additional balsa, increasing strength with minimal penalty in weight.

Torsion Webbing: The wing for this aircraft provided an uncommon structural challenge for the team due to our method of creating a wing that will fit another wing inside of it. With less central structure to the wing, it is more susceptible to torsion. The team employs cross torsion webbing across the bays to provide additional stiffness. The wing structure can be seen in Figure 6.1.



Figure 6.1: MSA wing in production.

Lightening Holes: The use of a concentrated and localized structure caused most structural members to not experience significant loading. Where possible, the team laser-cut lightening holes into ribs and bulkheads to reduce weight with little losses in the overall stiffness and strength of the aircraft.



Coating: Most balsa aircraft are coated with a heat shrink adhesive infused plastic covering material called Monokote, which is durable and easy to handle. However, the team chose to use a more delicate plastic covering, Ultracote, because it is significantly lighter.

Thermoforming: For the PA payload bay, the team had to choose between a balsa structure or thermoformed plastic. While the plastic shell is heavier, its increased durability and closer fit reduces risk during loading/unloading and decreases drag. These advantages made it the material of choice for the pod. The thermoforming mold is made from foam that is CNC machined and finish-sanded. An epoxy coat is applied to give it rigidity and resistance to temperature. This process is seen in Figure 6.2

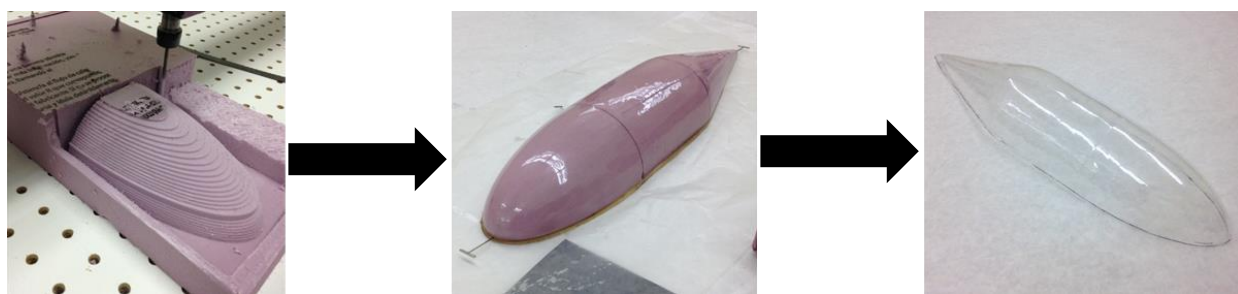


Figure 6.2: Manufacturing process of the thermoformed payload bay.

6.3 Manufacturing Milestones

A milestone chart was established at the beginning of aircraft manufacturing to ensure a logical, consistent order was followed during construction. Progress was recorded and monitored by the team leader to ensure all major milestones were met. The milestone chart is shown below in Figure 6.3, capturing the planned and actual timing of major events.

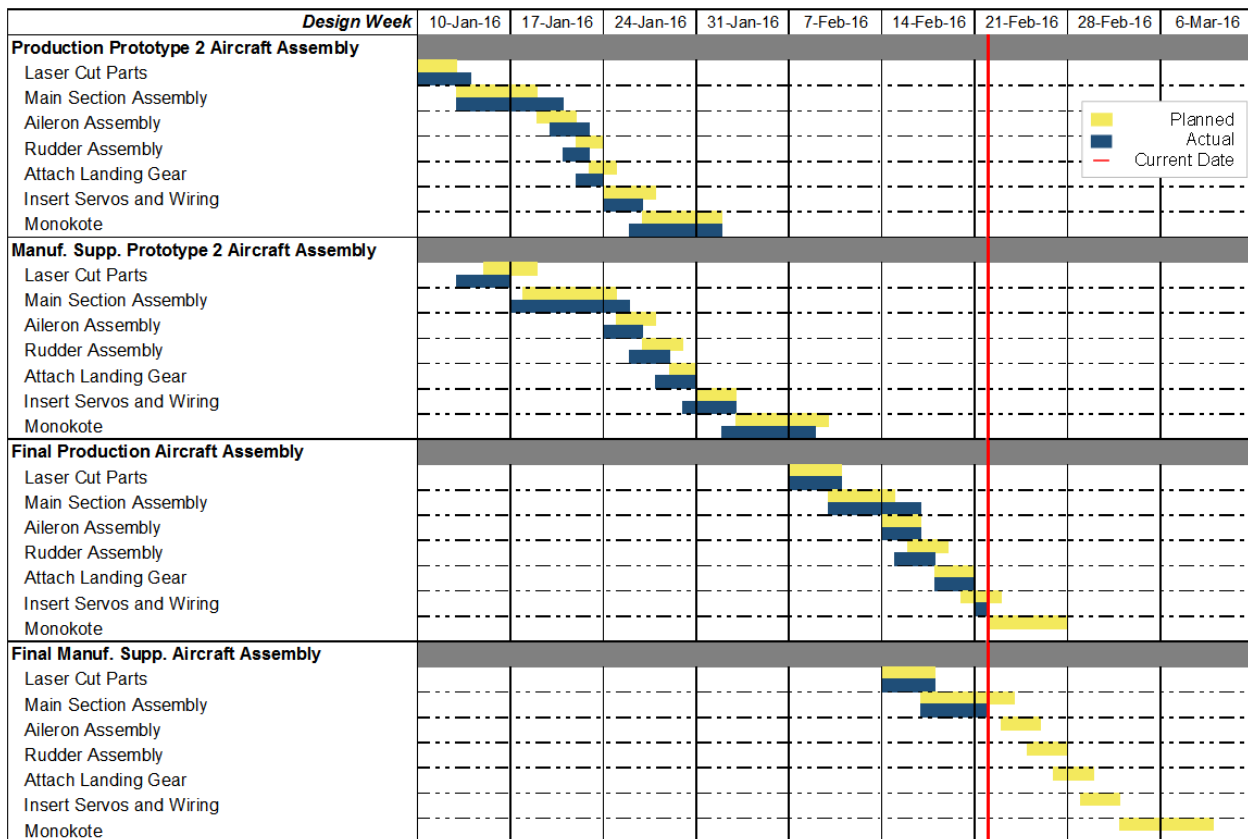


Figure 6.3: Aircraft manufacturing milestone chart showing planned and actual timing of objectives.

7. TESTING PLAN

A plan for an extensive testing campaign to validate the aircraft, and its components, was created to determine what configurations and subsystems would be the most capable. Testing culminates in test flying a full round of competition flights on the final competition airframe.

7.1 Objectives and Schedules

The testing was broken up into three main categories: propulsion, structures, and performance. The propulsion and structures subsystems were tested before flying the whole aircraft to gain knowledge and set realistic and useful objectives at each test flight. A breakdown of the testing schedule is displayed in the following Gantt chart, shown in Figure 7.1 below:

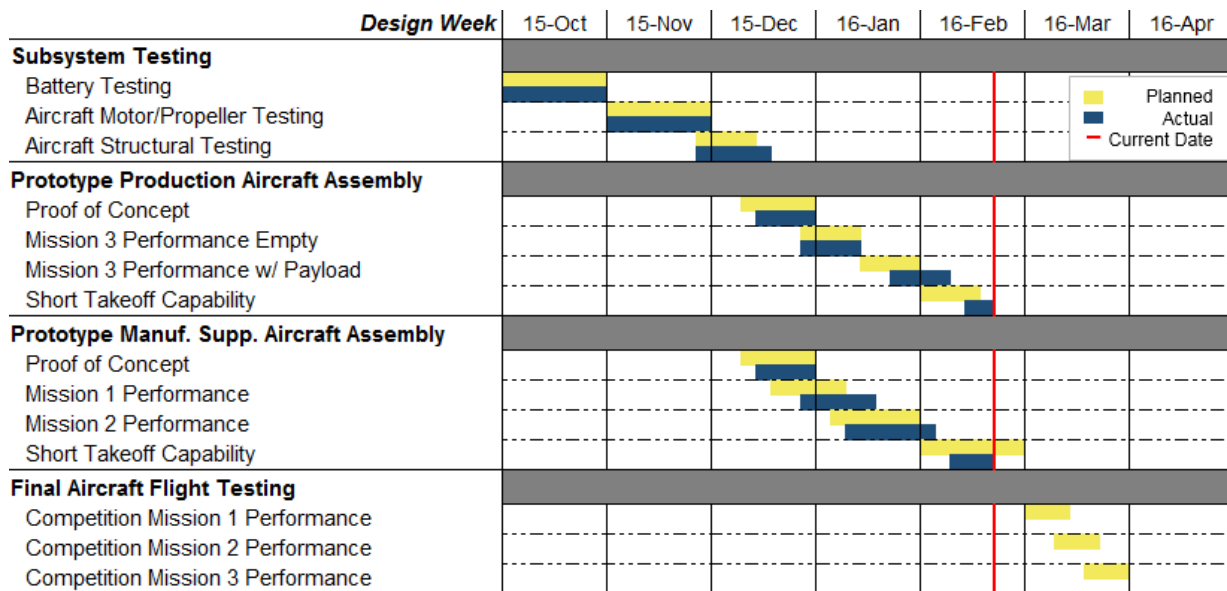


Figure 7.1: Aircraft and subsystem testing milestone chart showing planned and actual timing of objectives.

7.2 Propulsion Testing

The objectives for the propulsion testing were to determine which of the two motors would work best for both aircraft. The motors and propellers tested were based on MotoCalc predictions as expressed in Section 4.2. Thrust versus velocity for vehicle performance and power draw for motor performance for each motor propeller combination were determined using measurements of thrust, torque, RPM, voltage, and current draw. Using data obtained from testing, the team was able to compare the actual performance of the motors to the MotoCalc predictions in order to gather a better estimate of actual performance. This information allowed the team to select the best propulsion system to achieve the best score possible.

A rig that included load cells to calculate thrust and torque as well as an electric motor measurement system was constructed for the wind tunnel testing, and is shown in Figure 7.2. The team used the rig to perform static thrust tests and used the data to compare it with MotoCalc predictions. The electric motor parameters were monitored with an EagleTree system that records the RPM, voltage, and current draw of the motor. Custom written software was used to collect the torque and thrust values as well as to remotely control the motor for 30-second intervals with 10-second full thrust intervals and 10-second acceleration and deceleration intervals.

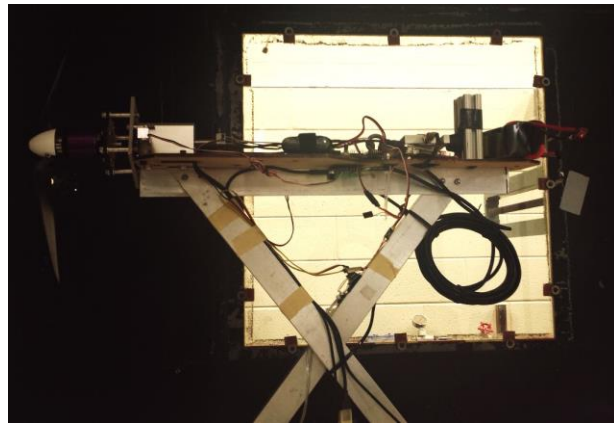


Figure 7.2: Picture of thrust test rig in wind tunnel.

The team will be utilizing the Georgia Tech Low Turbulence Wind Tunnel to conduct its wind tunnel tests. Due to time constraints and scheduling conflicts, the team has not tested within the tunnel as of when this report has been submitted but plans to do so in the near future. The wind tunnel is powered by a fan which forces air through a series of honeycombed grates creating a smooth, even flow of air. The fan creates airflow with a maximum airspeed of about 52 feet per second. The wind tunnel creates an environment closely resembling actual flight conditions and thus providing accurate motor and propeller efficiencies. The results of the static thrust tests are described in Section 8.1.

7.3 Integration of Production Aircraft into Manufacturing Support Aircraft

The system was designed to ensure the PA successfully fits within the MSA which splits into seven separate pieces. Prototypes were constructed to ensure successful operation. Assembly of the MSA around PA was tested in both the lab and flight field. Flight testing ensured the system functioned properly for Mission 2.

7.4 Structural Testing

To validate the design of the wings, the aircrafts were subjected to wing tip tests. A wing tip test simulates the maximum loading the wings would experience in flight by loading the payload bay with the maximum weight and lifting the plane by the wing tip. The tip test simulates a maneuver resulting in a root bending moment of 2.5g. This is shown in Figure 7.3.

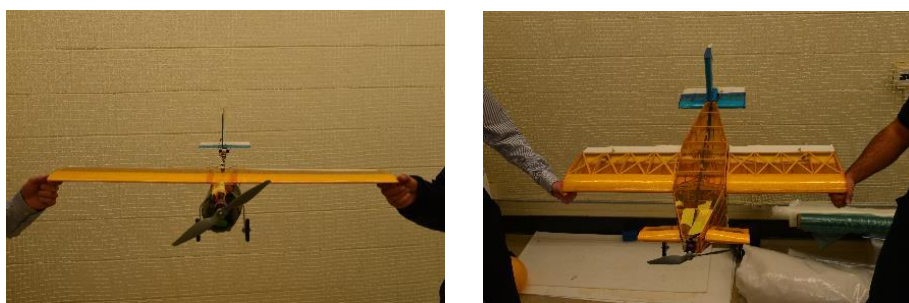


Figure 7.3: Wing tip loading test.



7.5 Flight Testing

Flight testing for both aircraft was conducted across two iterations, with a third planned as the final competition design. Initial iterations were used to determine the flying qualities of the aircraft designs. Verification of structural layouts and load estimates were also conducted. Missions were simulated and the necessary design modifications tabulated.

The second iterations are currently being used as testing platforms. Changes were made to the designs based on pilot and construction group feedback. For the PA, these included modifications to the wing structure and aileron size to make the plane lighter and easier to fit inside of the MSA. For the MSA, modifications included changes to the fuselage design to better mate with the tail and an increase in the main gear height to aid with takeoff and landing.

Currently, the second iteration of the PA is being used to verify the required battery size to complete M3. The second MSA frame is being used to test system M2 viability and determine further refinements to the design. Experience and data gained from all airframes will be used to improve the designs for a third iteration of both airframes that will go to competition. Both of the third iterations will fly simulations of their respective flight missions for proofing. The schedule and flight order is displayed in Table 7.1, seen below.

Table 7.1: Flight test goals and order for both aircraft.

Flight Test	Aircraft	Goal
1	First Iteration	Maiden flight
2	First Iteration	Takeoff distance
3	First Iteration	Mission runs
4	First Iteration	Mission runs
5	Second Iteration	Maiden flight
6	Second Iteration	Takeoff distance
7	Second Iteration	Motor performance testing
8	Second Iteration	Mission runs
9	Final Iteration	Maiden flight
10	Final Iteration	Mission runs

7.6 Checklists

Various tests have specific procedures which must be followed accurately to produce the desired objectives and ensure safety. This section lists the checklists utilized by *Buzzdryoshka* while conducting tests that required a significant amount of steps, such as propulsion and flight testing.



7.6.1 Propulsion Test Checklist

The checklist in Table 7.2 was created to ensure safety while dealing with propellers and electrical equipment, and to make sure the test is not wasted due to some mistake in preparation. This checklist was used in the testing of all motor, battery and propeller combinations.

Table 7.2: Propulsion testing checklist.

Propulsion Test Checklist								
1. Propeller secured?	<input type="checkbox"/>	2. Motor mount secured?	<input type="checkbox"/>	3. All plugs secured?	<input type="checkbox"/>			
4. Batteries peaked?	<input type="checkbox"/>	5. Throttle down?	<input type="checkbox"/>	6. Data system on?	<input type="checkbox"/>			
7. Custom code running?	<input type="checkbox"/>	8. All clear of testing rig?	<input type="checkbox"/>	9. Wind tunnel closed?	<input type="checkbox"/>			

7.6.2 Flight Test Checklist

The checklist in Table 7.3 was created with the important goal of preventing any system from malfunctioning in mid-air, which could lead to the aircraft crashing; its thorough execution is paramount to the team's success, and it will be used at the DBF event as well. ("P:" for PA and "M:" for MSA)

Table 7.3: Pre-flight checklist.

General System Checks										
Structural Integrity		Center of Gravity Location				Time		Date		
		X	P:	M:	Y	P:	M:			
Payload										
Laterally Secure?		Connections Secure?		Battery Pack		Receiver Pack		Payload Secure?		
P:	M:	P:	M:	P:	M:	P:	M:	P:		
Attachment secure?		Pins locked?		Clear of Jams?						
Control Surfaces										
Ailerons			Rudder			Elevator				
Deflects?	Glued?	Slop?	Deflects?	Glued?	Slop?	Deflects?	Glued?	Slop?		
P: M:	P: M:	P: M:	P: M:	P: M:	P: M:	P: M:	P: M:	P: M:		
Electronics and Propulsion										
Receiver Battery Charged?	Primary Battery Charged?	Receiver/Transmitter Go?		Wires secure?		Battery hot?		Prop secure?		
P: M:	P: M:	P: M:		P: M:		P: M:		P: M:		
Weather										
V_{wind}			Θ_{wind}			Temperature				
Initials for Approval										
Chief Engineer			Pilot			Advisor				



8. Performance Results

8.1 Component and Subsystem Performance

8.1.1 Propulsion

Batteries: A 10-cell, 1500mAh NiMH battery pack was discharged at 5 amps (3.3 times its capacity) and at 15 amps (10 times its capacity) to characterize the discharge capabilities of the NiMH batteries. The resulting data is shown in Figure 8.1 on a per cell basis. NiMH battery cells have a nominal voltage of 1.2V, and the 5 amp discharge curve is capable of maintaining this voltage. At 15 amps the cell voltage continuously drops, resulting in a small decrease in the available effective power. The higher current draw of the 15 amp discharge is necessary to achieve the power required for the aircraft.

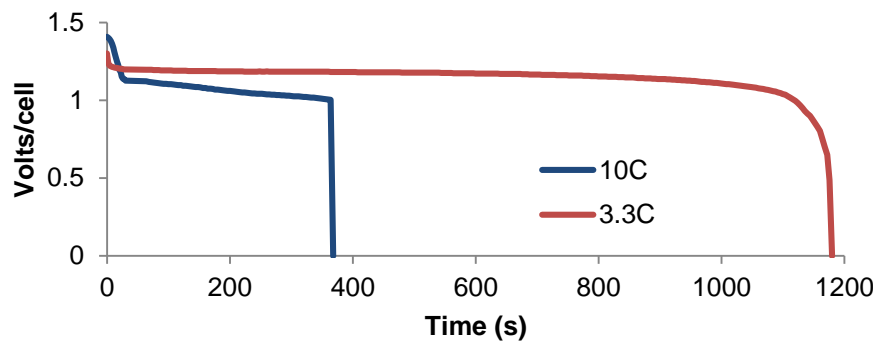


Figure 8.1: Battery discharge rates.

Motors and Propellers: The Cobra 2814/12 motor was tested using the MotoCalc software and the test stand as described in Section 7.2. Figure 8.2 shows the difference between the actual results and the theoretical results posed by the MotoCalc program for the propellers tested.

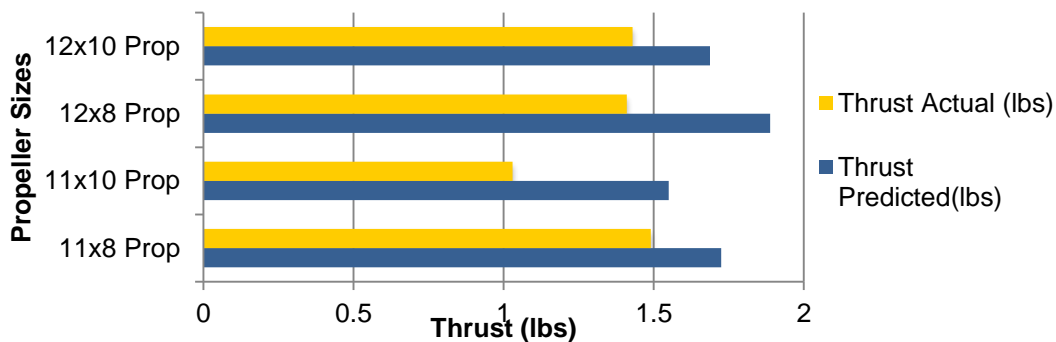


Figure 8.2: Difference between predicted thrust and actual thrust for different propellers.

Figure 8.2 shows that the 11x8 produces the greatest static thrust in the testing environment. This implies superior takeoff performance, leading the team to choose the 11x8 propeller.



8.1.2 Structural Tests

Wing Testing Results: The full size airplane was subjected to the required wing tip testing specified in the rules as part of the technical inspection process. This was done by loading the full internal Mission 2 payload of three blocks into the payload bay, then lifting the airplane by the wing tips. The successful wing tip test is shown in Figure 8.3.

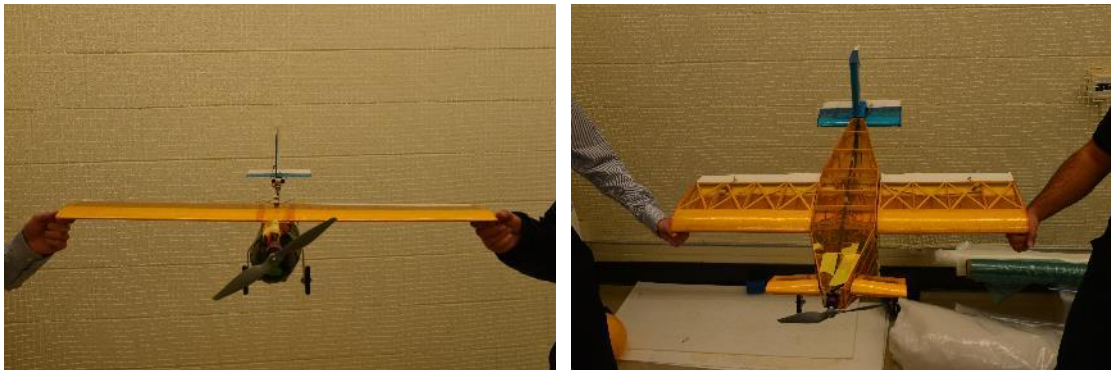


Figure 8.3: Wingtip structural test with full payload of the system.

8.2 System Performance

Testing of the system was conducted in the lab and at the flight field. Test results show that in both cases, assembly is found to be adequately simple and will not present complications during competition. The assembly time of the PA is fifteen seconds, including Gatorade bottle installation. The MSA is not restricted by an assembly time requirement, and fully encloses the PA. This is shown in Figure 8.4 below.



Figure 8.4: Exploded view of final assembled aircraft.



Flight tests of *Buzzedryoshka* were performed to evaluate the performance of the aircrafts and validate the performance predictions. To evaluate system performance during flight testing beyond simple lap timing and takeoff performance, the team equipped the aircraft with a data collection system that could be used to compare to the estimated mission performance in Section 5. The team purpose-built an Arduino-based telemetry system with a live data feed. On a number of test flights, the Arduino was mounted to the aircraft and recorded GPS at 1 Hz to yield trajectory data. An example of a full lap trajectory is displayed in Figure 8.5 superimposed on satellite imagery using Google Earth.



Figure 8.5: Trajectory of aircraft during competition laps from GPS data.

The results of flight testing are shown in Table 8.1. They indicate the performance predictions were optimistic. Further optimization and increasing pilot familiarity with the system should improve system performance to meet or exceed the predicted performance.

Table 8.1: Comparison of Predicted and Actual Performance Averages.

	1 st Lap Time (s)		Time for 360		Laps Flown		TOFL		Max. Speed	
	Pred.	Act.	Pred.	Act.	Pred.	Act.	Pred.	Act.	Pred.	Act.
M1	43.0	53.0	2.15	3.5	3	3	6.72	6.5	52.50	52.1
M2	47.2	78.0	4.26	4.0	1	1	20.7	40.0	51.80	51.3
M3	49.1	59.0	5.19	9.0	3	3	95.2	95.0	63.15	61.6

Lap times for M1, M2, and M3 vary significantly between the predicted and actual values. These differences are explained by the uncertainties in the predictions as described in Section 4.3.2. Namely, the mathematical models lack a vertical dimension and any wind model. Furthermore, they assume an ideal flight path, with the aircraft pushed to their performance limits during turns. In reality, the performance target of 3 laps in 5 minutes does not mandate flying the aircraft at the edge of their performance boundaries.



Predicted and actual times for a 360 degree turn are highly variable, again due to pilot behavior. In all cases, time for a 360 degree turn was predicted assuming maximum velocity. However, during testing, the pilot tended to reduce speed significantly when going into a turn, which reduced the turn radius. For M3, the discrepancy was due to the test pilot flying conservatively so as not to slip below stall speed.

Discrepancies between predicted and actual TOFL are low for M1 and M3, but high for M2. While M3 takeoff distance is currently within competition bounds, an increase in power to increase the safety margin is necessary. The M2 discrepancy is a result of differences between pilot actual behavior and assumed behavior. The model used for calculating TOFL assumes that the pilot immediately advances to maximum throttle, but the pilot has been taking off more conservatively to maintain ground steering. The M1 discrepancy is within bounds of error and likely arises due to occasional wind gusts.

The maximum flight speed predictions correlate well to the maximum speeds seen during flight tests. The model predicts this well, because it was written to simulate flight in the horizontal plane.

In summary, as of the time of this report, 21 flights of the PA and 10 flights of the MSA have been performed on two different prototypes of *Buzzedryoshka*. The research, component selection, and testing that fed into the design process resulted in a lightweight MSA capable of completing three laps for Mission 1, ferrying the PA for Mission 2, and flying three laps with the Gatorade bottle loaded in the PA for Mission 3. The concept of a single-engine, high wing, conventional system proved to be successful in completing the loading mission and all flight missions, and was proven through laboratory testing to be lighter than other designs of an equivalent power level. The *Buzzedryoshka* team is eagerly awaiting more testing opportunities to ensure success during all missions at the competition and hone pilot familiarity with the aircraft. The team is confident that the overall configuration for *Buzzedryoshka* as shown in Figure 8.6 will be victorious.

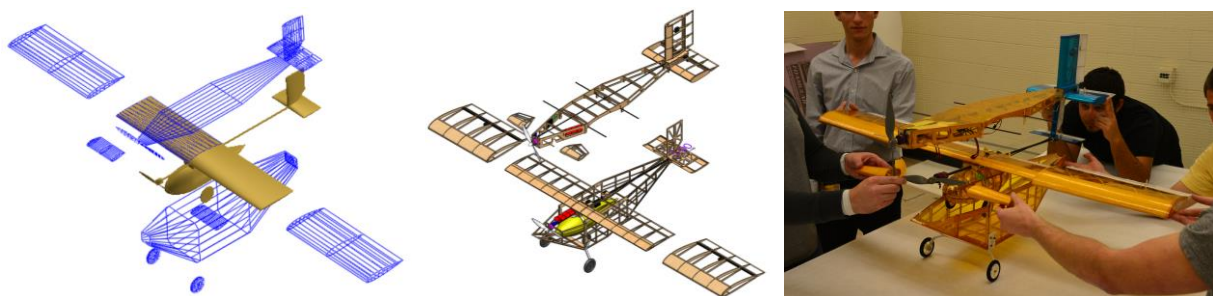


Figure 8.6: Progression from concept to reality of *Buzzedryoshka*.



9. REFERENCES

- Anderson. J. D. *Fundamentals of Aerodynamics*, 4th edition, McGraw Hill.
- Bauchau, O. A., & Craig, J. I. (January 7, 2009). *Aerospace Structural Analysis*. Springer.
- Drela, M., & Youngren, H. (2008, 08 04). *AVL*. Retrieved 01 10, 2009, from [http://web.mit.edu/drela/Public/web/avl/].
- Drela, M., & Youngren, H. (2008, 04 07). *XFOIL*. Retrieved 10 01 2008, from Subsonic Airfoil Development System: [http://web.mit.edu/drela/Public/web/xfoil/].
- Hoerner, Sighard F. *Fluid Dynamic Drag*. 2nd. Published by author, 1965.
- Katz, Joseph and Maskew, Brian. "Unsteady low-speed aerodynamic model for complete aircraft configurations," *Journal of Aircraft*. Vol. 25, pp. 302-310. Apr. 1988.
- McDaniel, Katie et al. (2008). *Georgia Institute of Technology Team Buzzed*. Editor: Johnson, Carl.
- Phillips, Warren F. *Mechanics of Flight*. 1st. Hoboken, NJ: Wiley, 2004.
- Roskam, Jan. *Airplane Design Part VI*. Darcorp, 2000.
- Roskam, Jan. *Airplane Flight Dynamics and Automatic Flight Controls Part I*. Darcorp, 2007.
- Selig, M. (2008, 02 19). *UIUC Airfoil Data Site*. Retrieved 10 01, 2008, from [www.ae.uiuc.edu/m-selig/ads.html].